University of Nebraska - Lincoln
DigitalCommons@University of Nebraska - Lincoln

Theses, Dissertations, and Student Research in Agronomy and Horticulture

Agronomy and Horticulture Department

8-2011

GATA-Family Transcription Factors in *Magnaporthe oryzae*

Cristian F. Quispe
University of Nebraska-Lincoln

Follow this and additional works at: https://digitalcommons.unl.edu/agronhortdiss

 Part of the Agricultural Science Commons, Agriculture Commons, Agronomy and Crop Sciences Commons, Bioinformatics Commons, Genetics Commons, Microbial Physiology Commons, Molecular Biology Commons, Molecular Genetics Commons, Other Cell and Developmental Biology Commons, Pathogenic Microbiology Commons, Plant Biology Commons, and the Plant Pathology Commons

Quispe, Cristian F., "GATA-Family Transcription Factors in *Magnaporthe oryzae*" (2011). *Theses, Dissertations, and Student Research in Agronomy and Horticulture*. 30.
https://digitalcommons.unl.edu/agronhortdiss/30

This Article is brought to you for free and open access by the Agronomy and Horticulture Department at DigitalCommons@University of Nebraska - Lincoln. It has been accepted for inclusion in Theses, Dissertations, and Student Research in Agronomy and Horticulture by an authorized administrator of DigitalCommons@University of Nebraska - Lincoln.

GATA-FAMILY TRANSCRIPTION FACTORS IN *MAGNAPORTHE ORYZAE*

by

Cristian Quispe

A THESIS

Presented to the Faculty of

The Graduate College at the University of Nebraska

In Partial Fulfillment of Requirements

For the Degree of Master of Science

Major: Agronomy

Under the Supervision of Professor Richard A. Wilson

Lincoln, Nebraska

August 2011

GATA-FAMILY TRANSCRIPTION FACTORS IN *MAGNAPORTHE ORYZAE*

Cristian Quispe, M.S.

University of Nebraska, 2011

Adviser: Richard A. Wilson

The filamentous fungus, *Magnaporthe oryzae*, responsible for blast rice disease, destroys around 10-30% of the rice crop annually. Infection begins when the specialized infection structure, the appressorium, generates enormous internal turgor pressure through the accumulation of glycerol. This turgor acts on a penetration peg emerging at the base of the cell, causing it to breach the leaf surface allowing its infection.

The enzyme trehalose-6- phosphate synthase (Tps1) is a central regulator of the transition from appressorium development to infectious hyphal growth. In the first chapter we show that initiation of rice blast disease requires a regulatory mechanism involving an NADPH sensor protein, Tps1, a set of NADP-dependent transcriptional inhibitors and the nonconsuming interconversion of NADPH and NADP acting as signal transducer.

The Tps1-dependent Nmr inhibitor proteins regulate the activity of GATA-family transcription factors that are involved in several essential aspects of the life style of the fungus. Thus, We elucidated that the GATA transcription factor Asd4 is

essential for pathogenicity and is a positive regulator of appressorium development and sporulation, in contrast to the GATA transcription factor Pas1 that is a negative regulator of appressorium development and sporulation.

In chapter two, we set out to understand the specific role of the GATA transcription factor Asd4. We show that Asd4 controls the activation of the Tor kinase pathway, which is essential for virulence and integrates important processes such as regulation of transcription, translation, ribosome biogenesis, trafficking and regulation of Golgi, secondary metabolism, autophagy and nitrogen metabolism. This mechanism is essential to the initiation of infection-associated autophagy during plant infection and during *in planta* invasion.

In summary, in this study we characterized two essential regulators, Tps1 and Asd4, in *M. oryzae*, and we believe that understanding the regulatory mechanisms that allow the fungus to cause disease may provide new means to control the rice blast pathogen and play an important role in ensuring global food security in the future.

ACKNOWLEDGEMENTS

I would like to thank my advisor, Dr. Richard Wilson, for giving me the opportunity, intellectual support, encouragement and freedom for working in my thesis during the last two years.

I am also very grateful to Dr. James Van Ettan, Dr. Kenneth Nickerson and Dr. Steve Harris, members of my Academic Committee, for their constructive critics during the development of my research. Dr. James Steadman, Margaret, Mary Jo and Joann for the great administrative support.

I wish to thank my friends at UNL for the unforgettable moments: Katty, Anita, Leny, Justin, Eric, Daniela, Oscar, Angel, Yamira, Jorge, Leandro, Luis, Irina, Han, Jim. Thanks to Pat, Marlene, and Becky, for their valuable help and encouragement during my time on the Plant Science Building. Thank you to my great family from the Zamorano Collage: Alejandra, David, Eileen, Elizabeth, Christian, Henry.

I would like to thank my family for all of their love and faith: Ligia, Lorena, Catherine.

Finally, special thanks go to Anya Seng, my valuable and beautiful labmate, without her I could not be writing this words. Memories of our “having fun” phrase will remind forever, thank you for your hard work on mornings and nights.

DEDICATION

All my love and dedication to Ligia Quitiguina. She has been able to encourage me every day to continue in this adventure.

TABLE OF CONTENTS

LIST OF FIGURES

Chapter ONE

Chapter TWO

LIST OF TABLES

Chapter ONE

An NADPH-dependent genetic switch regulates plant infection by the rice blast fungus

Reference:

Wilson RA, Gibson RP, Quispe CF, Littlechild JA, Talbot NJ. 2010. An NADPH-dependent genetic switch regulates plant infection by the rice blast fungus. Proc Natl Acad Sci U S A. 14;107 (50):21902-7.

ABSTRACT

To cause rice blast disease, the fungus *Magnaporthe oryzae* breaches the tough outer cuticle of the rice leaf using specialized infection structures called appressoria. These cells allow the fungus to invade the host plant and proliferate rapidly within leaf tissue. Here, we show that a novel NADPH-dependent genetic switch regulates plant infection in response to the changing nutritional and redox conditions encountered by the pathogen. The biosynthetic enzyme trehalose-6-phosphate synthase (Tps1) integrates control of glucose-6-phosphate metabolism and nitrogen source utilization by regulating the oxidative pentose phosphate pathway, the generation of NADPH, and the activity of nitrate reductase. We report that Tps1 directly binds to NADPH and thereby regulates a set of related transcriptional co-repressors, comprising three proteins, Nmr1, Nmr2 and Nmr3, which can each bind NADP. Targeted deletion of any of the Nmr-encoding genes partially suppresses the non-pathogenic phenotype of a Δ*tps1* mutant. Tps1-dependent Nmr corepressors control the expression of a set of virulence-associated genes, that are de-repressed during appressorium-mediated plant infection. When considered together, these results suggest that initiation of rice blast disease by *M. oryzae* requires a regulatory mechanism involving an NADPH sensor protein, Tps1, a set of NADP-dependent transcriptional corepressors and the non-consuming interconversion of NADPH and NADP acting as signal transducer.

Key words: fungal pathogenicity, ascomycete, cofactor

INTRODUCTION

Rice blast disease represents a significant constraint on worldwide rice production, resulting in severe epidemics and overall global yield losses of 10-30% each year (1). Rice constitutes 23% of the calories consumed annually by the global human population, so understanding and controlling rice blast disease could play an important role in ensuring global food security in the future (2). To infect rice plants, the blast fungus *Magnaporthe oryzae* produces specialised infection cells called appressoria, which rupture the leaf cuticle and allow fungal hyphae to invade and colonize the host. The fungus is able to proliferate rapidly within rice cells, deriving nutrition from living tissue while evading or suppressing plant defenses (1). Understanding the regulatory mechanisms that allow the fungus to undergo these developmental transitions and to grow so effectively within its host may provide new means to control rice blast disease.

In this study we set out to investigate the gene regulatory mechanisms that condition the ability of *M. oryzae* to respond to the nutrient status of its environment during plant infection– moving from the nutrient-free conditions of the rice leaf surface to the relatively nutrient-rich interior of the leaf. Previously, we observed a pivotal role for the biosynthetic enzyme trehalose-6-phosphate synthase (Tps1) in the regulation of carbon and nitrogen metabolism in *M. oryzae* (3, 4). Tps1 is required for production of the non-reducing disaccharide trehalose from glucose-6-phosphate (G6P) and (UDP)-glucose (3). Mutants lacking Tps1 are able to produce appressoria, but these cells do not function correctly and the fungus cannot colonize rice tissue (3). A Δ*tps1* gene deletion mutant

does not produce trehalose, or the intermediate trehalose-6-phosphate (T6P), but by introducing mutations to the G6P binding pocket of Tps1, we showed that impairment of pathogenicity in *M. oryzae* by Δ*tps1* strains is not due simply to loss of trehalose biosynthesis. Introducing amino acid substitutions into Tps1, which prevent G6P-binding, rendered the fungus non-pathogenic, while mutations which solely affected the catalytic activity of the enzyme did not affect its role in rice blast disease, suggesting that the inability of Δ*tps1* mutants to sense intracellular G6P may be associated with their loss of virulence (4).

Tps1 appears to integrate control of both carbon and nitrogen metabolism in *M. oryzae* because without the ability to sense G6P, Δ*tps1* mutants are unable to grow on nitrate as a sole source of nitrogen. Filamentous fungi carry out nitrate reduction to ammonium via the sequential reactions of nitrate reductase (NR) and nitrite reductase. NADPH provides the reducing power for the first step of this pathway and is a co-factor for NR. In *M. oryzae*, growth on nitrate normally results in increased hexokinase (Hxk1) activity and a rise in G6P production compared to growth on ammonium as nitrogen source (4). Because both G6P dehydrogenase (G6PDH) activity and NADPH levels are significantly reduced in Δ*tps1* mutants, we reasoned that sensing of G6P by Tps1 might lead to increased NADPH production in the oxidative pentose phosphate pathway (PPP) via activation of G6P dehydrogenase (G6PDH), thus ensuring that sufficient reducing power (in the form of NADPH) is available to NR to allow growth of the fungus on nitrate. Consistent with this idea, Δ*tps1* mutants are depleted for NADPH and lack the reducing power to metabolize nitrate as a nitrogen source (4). We could not, however, determine

the precise mechanism that allowed Tps1 to exert such a profound effect on the establishment of rice blast disease based solely on its role as a metabolic regulator.

In this report we show that the virulence-associated function of Tps1 is mediated by a family of NADP-dependent transcriptional co-repressors, linking its metabolic function to a wider role in the control of gene expression. This transcriptional regulatory mechanism involves the interaction of up to three GATA-factor transcriptional activators with cognate NADP-binding corepressors and is necessary for regulation of a set of genes that are expressed during appressorium-mediated plant infection in *M. oryzae*. Furthermore, we demonstrate that Tps1 directly binds NADPH, consistent with the operation of a novel NADPH-dependent genetic switch that allows the rice blast fungus to regulate gene expression in response to rapidly fluctuating changes in nutrient and redox status during plant infection.

RESULTS

Tps1 regulates nitrogen source utilization through the oxidative pentose phosphate pathway

We initially set out to investigate the mechanism by which *M. oryzae* Tps1 regulates nitrogen source utilization and to determine whether this was important for its role in rice blast disease. Tps1 is essential for *M. oryzae* to grow on nitrate as a sole nitrogen source and we therefore needed to establish whether nitrate metabolism was necessary for fungal virulence. Previous studies (5, 6) provided some evidence that the wide domain regulator of nitrogen source utilization was dispensable for virulence. To test this in a more

systematic manner, we independently generated targeted deletion mutants for the structural gene for nitrate reductase (*NIA1*), the pathway specific activator of *NIA1* gene expression (*NIR1*) and the wide domain GATA factor (*NUT1*), as shown in Supplemental Information (Fig. S1). All of the mutants were still able to cause rice blast disease symptoms, although lesions were reduced in size compared to those caused by the isogenic wild type strain Guy11. This suggests that the role of Tps1 in regulating nitrate metabolism is not the primary reason for its significance in fungal pathogenicity.

Tps1 appears to exert its effect on nitrate reductase because of its function in G6P sensing by Tps1 and its modulation of NADPH production through the oxidative pentose phosphate pathway (PPP). In Δ*tps1* mutants, G6PDH activity is reduced during vegetative growth on nitrate compared to Guy11, which is accompanied by a significant reduction in NADPH levels (4). To investigate the relationship directly, we used quantitative real time PCR (qPCR) and observed a 9-fold reduction in *G6PDH* gene expression in a Δ*tps1* mutant compared to the wild type during growth on nitrate (Fig. S2*A*). Moreover, *G6PDH* was expressed 12-fold more highly in wild type appressoria compared to conidia (Fig. S2*B*), suggesting that G6PDH levels might be particularly important during appressorium-mediated plant infection. To test this idea, we overexpressed the *G6PDH* gene in a Δ*tps1* mutant of *M. oryzae*. Using qPCR, we found that the *M. oryzae* β-tubulin-encoding gene was 60-fold more highly expressed than *G6PDH* in a Δ*tps1* mutant strain exposed to nitrate (Fig. S2*C*). We therefore fused the *G6PDH* gene coding sequence to the β-tubulin gene promoter and introduced this into a

Δ*tps1* mutant. In a resulting transformant, G6PDH activity was increased 260.4 ± 5 % when the fungus was switched to nitrate-containing medium.

Interestingly, overexpression of *G6PDH* in a Δ*tps1* mutant background partially restored the ability to cause rice blast disease in a susceptible cultivar, CO-39, as shown in Fig. 1*A* We conclude that elevation of G6PDH activity, which consumes G6P and generates NADPH, can at least partially compensate for the loss of trehalose-6-phosphate synthase in Δ*tps1* mutant of *M. oryzae*.

Tps1 can directly bind NADPH

As a result of the importance of G6PDH activity in the generation of NADPH we wondered whether Tps1 might be directly regulated by the ratio of NADP/NADPH. We therefore purified recombinant Tps1 protein and titrated it against NADPH to establish whether Tps1 was able to bind the cofactor. A specific interaction between Tps1 and NADPH was detected, as monitored by a quenching of NADPH fluorescence at 465 nm in the presence of increasing concentrations of Tps1 (Fig. 1*B*). Furthermore, we found evidence that NADPH could be displaced from Tps1 by the presence of G6P because the Tps1-mediated reduction in NADPH fluorescence could be reversed by addition of excess G6P, as shown in Fig. 1*C*. We investigated the specificity of NADPH binding in more detail by measuring the intrinsic tryptophan fluorescence of Tps1 in the presence or absence of NAPDH. Figure S3*A* demonstrates the tryptophan quenching occurs in the active site of Tps1 in the presence of NADPH. From these data, the calculated Hill coefficient, used to determine the dissociation constant for a substrate bound to a macromolecule, gave a binding constant of 3.96 +/- 0.06 μM and a Hill slope of 5.18 +/-

0.35. This value is consistent with cooperative binding and demonstrates that binding of NADPH by Tps1 is a specific interaction. The high Hill coefficient for Tps1 and NADPH also implies that although only one molecule is present in the active site of each protein, NADPH binding might promote higher-order protein conformations, such as Tps1 tetramers. Using our modelled structure of Tps1, based on the solution structure of the bacterial Tps1 homologue otsA (4), we sought a structural explanation of the interaction of NADPH with Tps1. The native substrates of Tps1, UDP-glucose and G6P, when modelled into the Tps1 active site have calculated energies of binding of -19 kcal/ mol and -14 kcal/ mol respectively, as shown in Fig. 1*D*. NADPH can, however, also be modelled into the active site with a calculated energy of binding of -27 kcal/ mol (Fig. 1*D*). The structural similarity between NADPH and the native Tps1 substrates, coupled with the similarity in predicted energies of binding, is consistent with a mechanism whereby NADPH can reversibly displace G6P and UDP-glucose from the Tps1 active site to inhibit Tps1 activity during conditions of elevated NADPH levels. Conversely, when NADPH is consumed by NADPH-requiring enzymes (such as NR), G6P and UDP-glucose can displace NADPH at the active site, and, through G6P sensing, activate NADPH production by G6PDH. This is consistent with a feedback loop model controlling Tps1-dependent G6PDH activity in response to available G6P and NADPH.

Identification and functional characterization of NADP-dependent Nmr co-repressors

To investigate how a Tps1/NADPH-dependent regulatory process might regulate fungal virulence, we next investigated how Tps1 regulates gene expression. Δ*tps1* mutants do

not express the NR-encoding gene *NIA1* when exposed to nitrate and instead adopt an ammonium-responsive status (including the expression of genes encoding ammonium transporters), irrespective of the nitrogen source to which the fungus is exposed (Fig. S4*A*). In filamentous fungi, such as *Aspergillus nidulans* and *Neurospora crassa*, the presence of ammonium represses the expression of genes encoding enzymes to metabolise alternative nitrogen sources (7). This is due in part to a repressor protein NmrA/Nmr1, which prevents the activity of a GATA-factor transcription factor, AreA/Nit2, the central regulator of gene expression when ammonium is depleted (4). We therefore reasoned that in *M. oryzae*, Tps1-dependent transcriptional regulation of *NIA1* is likely to be mediated via control of the equivalent areA/Nit2-like transcription factor (TF), Nut1, by the repressor Nmr1 (ref. 4 and Fig. S4*A*). In contrast to previously characterized free-living fungal species, however, the genome of *M. oryzae* has two additional homologues of *NMR1* (*NMR2* and *NMR3*) (8), as shown in Fig. S4*B*. Low stringency yeast two-hybrid analysis, using β-galactosidase activity as the detection assay, provided evidence of a physical interaction between Nmr1 and Nmr3 with Nut1, suggesting that two of the *M. oryzae* Nmr proteins are functional homologues of NMRA (Fig. 2). To test the role of these genes in Tps1 regulation, we deleted *NMR1*, *NMR2* and *NMR3* in a Δ*tps1* mutant background. Strikingly, targeted deletion of *NMR1*, *NMR2* or *NMR3* all partially restored the ability of the Δ*tps1* mutant to cause rice blast disease (Fig. 2). No significant differences in lesion number were observed between leaves inoculated with the wild type and Δ*tps1* Δ*nmr* suppressor strains (Fig. 2*B*), but relative lesion sizes were reduced in Δ*tps1* Δ*nmr1* (mean relative lesion size = 49 ± 22 pixel^2, n =

12 leaves), Δ*tps1* Δ*nmr2* (30 ± 19 pixel^2, n = 13) and Δ*tps1* Δ*nmr3* (19 ± 7 pixel^2, n = 25) compared to Guy11 (109 ± 33 pixel^2, n = 12). By contrast, deletion of the *NMR* genes singly, or together, in a wild-type strain did not significantly affect fungal pathogenicity (Fig. S4*C*). Deletion of the *Nmr* genes also resulted in partial derepression of nitrate reductase activity in wild type and Δ*tps1* mutant (see Fig. S4*D* and Fig. S4*E*) and partial remediation of sporulation of Δ*tps1* strains on nitrate media (Fig. S4*F*). However, although partially remediated for virulence, Δ*tps1* Δ*nmr3* suppressor strains were not restored for sporulation on nitrate media (Fig. S4*F*). This indicates that the regulation of virulence-associated gene expression by Nmr proteins is both complex and independent of nitrate utilization.

We can therefore conclude that the three Nmr proteins act as corepressors to control virulence-associated gene expression downstream of Tps1. Low-stringency yeast 2-hybrid studies did not detect a physical interaction between the Nmr proteins and Tps1 (Fig. 2*C*), suggesting that direct modulation of Nmr activity by Tps1 is unlikely. However, each Nmr protein possesses a putative NADP-binding Rossman fold, which has been shown in *A. nidulans* NMRA to bind NADP (9) (Fig. S4*B*). We therefore investigated the role of NADP-binding in Nmr function and Tps1 regulation in *M. oryzae*. Focusing on Nmr1, we found that introducing a native copy of *NMR1* into a Δ*tps1* Δ*nmr1* double mutant complemented the *Δnmr1* gene deletion, as expected, and resulted in strains that, like Δ*tps1* single mutants, were non-pathogenic (Fig. 2). However, we also constructed a mutant allele of *NMR1* encoding a T13V substitution. This change has been shown in *A. nidulans* NmrA and *Dictyostelium discoideum* PadA, to impair

NADP-binding (10, 11). Expression of the *NMR1*^{T13V} allele in a Δ*tps1* Δ*nmr1* double mutant did not restore the Δ*tps1* non-pathogenic phenotype (Fig. 2*D*). We conclude that the nonpathogenic mutant phenotype of Δ*tps1* mutants is associated with the role of Nmr1, Nmr2 and Nmr3 in repressing virulence-associated gene expression. We can also infer that the function of Nmr1 to carry out this role depends on its ability to bind NADP.

Tps1-dependent gene expression is modulated by the presence of Nmr co-repressors

To understand how Tps1 might control virulence-associated gene expression during plant infection, we carried out comparative gene expression analysis of the wild type, Δ*tps1* mutant and the Δ*tps1*Δ*nmr1*, Δ*tps1*Δ*nmr2*, and Δ*tps1*Δ*nmr3* suppressor strains. During vegetative growth on nitrate compared to ammonium, we found that two known virulence genes *MPG1* and *ALB1* (12, 13), six genes encoding putative NADPH-dependent enzymes (*NIA1*, *ALD1, KEF1, SDY1, OXD1 and OYE1*), and a putative metalloprotease (*MPT1*) were expressed in a Tps1-dependent manner in response to nitrate (Fig. 3*A* and 3*B*, Table S1 and Fig. 3S*A*). Expression of these genes was at least partially restored in the Δ*tps1*Δ*nmr1*, Δ*tps1*Δ*nmr2* or Δ*tps1*Δ*nmr3* suppressor strains compared to the Δ*tps1* mutant, suggesting they are controlled via NADP-dependent Nmr inhibition of transcription (Fig. 3*C*). In addition, we found that G6PDH gene expression was also elevated in the Δ*tps1*Δ*nmr1*, Δ*tps1*Δ*nmr2* and Δ*tps1*Δ*nmr3* suppressor strains, compared to the Δ*tps1* mutant, during growth on nitrate (Fig. 3*D*). *G6PDH* and a subset of the genes analyzed in Fig. 3*C* were elevated in expression during appressorium development, consistent with the operation of this regulatory mechanism during plant infection (Fig. S2*B* and Fig. 3*E*). Moreover, some genes, like *ALB1* and *G6PDH*, were derepressed in

the Δ*tps1*Δ*nmr1*, Δ*tps1*Δ*nmr2* and Δ*tps1*Δ*nmr3* suppressor strains compared to Δ*tps1*, while other genes are derepressed in some suppressor strains but not others. The expression of *ALD1*, for instance, was only affected in the Δ*tps1*Δ*nmr2* mutant. This suggests that Nmr corepressor may work either individually or cooperatively to regulate gene expression, and this may result from their regulation of additional GATA-factors. Consistent with this idea, a subset of the genes were expressed in a *NUT1* dependent manner (Fig. 3*A*), while others were expressed independently of *NUT1* (Fig. 3*B*), indicating that the Nmr proteins may indeed regulate other GATA family transcription factors. To test this idea, we carried out high stringency yeast two-hybrid experiments to determine whether Nmr proteins can interact with other GATA family transcription factors including Asd4, a putative homologue of a *Neurospora crassa* morphogenetic regulator (14); Pas1, a GATA factor containing a pas-fold domain involved in redox (15) and/ or light sensing, which is a putative homologue of white collar-2 from *N. crassa* (8); and Sre1, a GATA factor required for siderophore metabolism (16). We found evidence that the Nmr1, Nmr2 and Nmr3 can physically interact with Asd4, while Nmr2 interacts with Pas1, as shown in Fig. 4*A*. No interaction was observed with Sre1. Based on their potential interaction with Nmr co-repressors, we decided to investigate the function of *ASD4* and *PAS1*. We carried out targeted gene replacements and found that Δ*asd4* mutants displayed reduced hyphal growth (Fig. S5*A*) and sporulation. By contrast, Δ*pas1* mutants showed enhanced conidiation (Fig. S5*B*). Significantly, Δ*asd4* mutants were unable to cause rice blast disease (Fig. 4*B*) which was associated with their inability to form appressoria (Fig. S5*C*).

We conclude that Tps1 affects virulence-associated gene expression via its modulation of a set of NADP-dependent transcriptional repressors, which target GATA factors implicated in both fungal development and pathogenicity.

DISCUSSION

In this study we set out to understand the role of trehalose-6-phosphate synthase as a key regulator in the establishment of rice blast disease (4). When considered together, our results are consistent with a role for Tps1 as part of an NADPH-dependent genetic switch in *M. oryzae*, which is essential for virulence and integrates the intracellular monitoring of nutritional and redox status with control of fungal gene expression. At the heart of this regulatory mechanism is the nonconsuming interconversion of NADPH and NADP, which bind to Tps1 and the Nmr transcriptional co-repressor proteins, respectively, as shown in the model presented in Fig. 4*C*. Nmr proteins interact with at least three GATA family transcription factors to regulate expression of genes necessary for virulence, in addition to a number of genes encoding putative NADPH-dependent enzymes. The switch has two distinct modes, an “on” and a default “off” status, depending on the nutrient condition of the fungal cell. When G6P is available and the NADPH/NADP ratio is high, the switch is “on” and dynamically links G6P availability to gene expression with *(i)* NADPH depletion by enzymes such as nitrate reductase (NR) being balanced by Tps1-dependent NADPH production in response to G6P sensing, *(ii)* NADPH production and G6P consumption maintained in equilibrium by competition for Tps1-binding, and *(iii)* the expression of virulence-associated genes and genes encoding NADPH-requiring

enzymes, such as NR, induced only under NADPH replete conditions due to inactivation of the Nmr corepressors resulting from low levels of NADP. Trehalose would also be produced as a storage compound under these conditions. However, when G6P levels and the NADPH/NADP ratio are low, the system cannot maintain dynamic equilibrium. Tps1 becomes inactive because it cannot bind either NADPH or its native substrates. G6PDH activity and gene expression is reduced, and the default "off" position of the pathway is therefore NADP-activation of the Nmr corepressor proteins. Further feedback to the system is provided by the likely control of *G6PDH* gene expression exerted by the GATA factor/Nmr transcriptional regulators. The default "off" position is also seen in Δ*tps1* mutants, because the Nmr proteins are constitutively active, repressing virulence-associated gene expression.

The involvement of dinucleotide cofactors in transcriptional regulation has not been widely reported, but was recently predicted from a study in *Saccharomyces cerevisiae* where NAD(P) was shown to have the potential to act as a co-factor in the interaction between Gal80p and Gal4p during induction of galactose metabolism (17). In mammals, meanwhile, a family of histone deacetylases, the sirtuins, are involved in regulation of diverse cellular processes, and appear to be dependent on NAD for their activity (reviewed in 18), ensuring a tight link between sirtuin activity and the underlying metabolic status of the cell. However, the results presented here suggest that *M. oryzae* Tps1 acts as part of an NADP(H) homeostatic model, where the expression of genes encoding NADP(H)-requiring enzymes directly influences NADPH production and corresponding gene expression. We speculate that this adaptability to fluctuating

nutritional environments may be key to the success of plant pathogens such as *M. oryzae* which must quickly adapt from nutrient-free leaf surfaces to intracellular propagation within living plant tissue. Once in the plant the fungus must, for instance, undergo rapid genetic re-programming in order to elaborate specialized invasive hyphae from the thin penetration hyphae, and evade or suppress the host defense response to establish disease (19). The Tps1 genetic switch described in this study may be responsible for postpenetration genetic reprogramming because Δ*tps1* strains form appressoria but these are unable to develop into invasive hyphae to establish disease (3). Significantly, T6P synthases have been shown to have important roles in developmental biology in an increasing range of organisms, being necessary for plant embryonic development, flowering and other morphogenetic processes (20). This suggests that the genetic mechanism defined in this study may be a more widespread mechanism for integrating metabolic and genetic regulation during eukaryotic development.

MATERIALS AND METHODS

Fungal Strains, Growth Conditions, and DNA Analysis

M. oryzae strains used in this study are derived from Guy11 (1,3,4). Standard procedures of *M. oryzae* growth, maintenance, appressorium formation and transformation were performed, as described previously (12). Rice plant infections were performed as described previously (12). DNA and RNA extractions were as described in Ref. 4. Nucleic acid quantity and purity was ascertained on a NanoDrop Spectrophotometer (Lab Tech International). Gel electrophoresis, restriction enzyme digestions, DNA ligations and PCR were performed using standard procedures (21).

Transcript and protein analysis

cDNA synthesis and qRT-PCR was performed as described in Supplementary Materials and Methods. Yeast two-hybrid analysis was performed using the Matchmaker™ GAL4 Two-Hybrid System 3 kit from Clontech. Purified Tps1 recombinant protein was obtained using the *Arcticexpress™* (Stratagene) gene expression system. Whole cell protein extraction and the nitrate reductase activity assays were performed as described previously (4). Activities were determined on a Pharmacia Biotech spectrophotometer in triplicate. All assay components were purchased from Sigma, except NADPH (Calbiochem). NADPH fluorescence was recorded on a 200 series microplate reader (Tecan Group Ltd). Protein modelling of *M. oryzae* Tps1 was performed as described in Supplementary Materials and Methods. Statistics were performed using *student's t-test.* Protein sequence alignments were performed using ClustalW and illustrated using BoxShade.

Generation of *M. oryzae* gene deletion mutants

Targeted gene replacement of *M. oryzae* genes were performed based on the split marker strategy (22), as described in Supplementary Materials and Methods and Fig. S4. *M. oryzae* gene sequence information was acquired from http://www.broad.mit.edu/annotation/genome/magnaporthe_grisea/MultiHome.html. For full experimental protocols, see Supplementary Methods and Methods.

REFERENCES

1. Wilson RA, Talbot NJ (2009) Under pressure: investigating the biology of plant infection by the rice blast fungus *Magnaporthe oryzae. Nature Rev Microbiol.* 7: 185-195.

2. Pennisi E (2010) Armed and Dangerous *Science* 327: 804-805.

3. Foster AJ, Jenkinson JM, Talbot NJ (2003) Trehalose synthesis and metabolism are required at different stages of plant infection by *Magnaporthe grisea*. *EMBO J* 22: 225-235.

4. Wilson RA, Jenkinson, JM, Gibson, RP, Littlechild, JA, Wang, ZY, Talbot, NJ (2007) Tps1 regulates the pentose phosphate pathway, nitrogen metabolism and fungal virulence. *EMBO J* 26: 3673-3685.

5. Froeliger E H, Carpenter BE (1996) NUT1, a major nitrogen regulatory gene in *Magnaporthe grisea*, is dispensable for pathogenicity. *Mol Gen Genet* 251: 647-656.

6. Lau G, Hamer JE (1996) Regulatory Genes Controlling MPG1 Expression and Pathogenicity in the Rice Blast Fungus *Magnaporthe grisea*. *Plant Cell* 8: 771-781.

7. Wilson RA, Arst HN, Jr (1998) Mutational analysis of AREA, a transcriptional activator

mediating nitrogen metabolite repression in *Aspergillus nidulans* and a member of the "streetwise" GATA family of transcription factors. *Microbiol Mol Biol Rev* 62: 586-596.

8. Dean R A *et al.* (2005) The genome sequence of the rice blast fungus *Magnaporthe grisea*. *Nature* 434: 980-986.

9. Lamb HK, Leslie K, Dodds AL, Nutley M, Cooper A, Johnson C, Thompson P, Stammers DK, Hawkins, AR (2003) The Negative Transcriptional Regulator NmrA Discriminates between Oxidized and Reduced Dinucleotides. *J Biol Chem* 278: 32107–32114.

10. Lamb HK, Ren J, Park A, Johnson C, Leslie K, Cocklin S, Thompson P, Mee C, Cooper A, Stammers DK, Hawkins A R (2004) Modulation of the ligand binding properties of the transcription repressor NmrA by GATA-containing DNA and site-directed mutagenesis. *Protein Sci* 13: 3127-3138.

11. Nunez-Corcuera B, Serafimidis I, Arias-Palomo E, Rivera-Calzada A, Suarez T (2008) A new protein carrying an NmrA-like domain is required for cell differentiation and development in *Dictyostelium discoideum*. *Dev Biol* 321: 331-342.

12. Talbot N J, Ebbole DJ, Hamer JE (1993) Identification and characterization of MPG1, a gene involved in pathogenicity from the rice blast fungus *Magnaporthe grisea*. *Plant Cell* 5: 1575-1590.

13. Chumley FG, Valent B (1990) Genetic analysis of melanin deficient non-pathogenic mutants of *Magnaporthe grisea. Mol. Plant Microbe Interact* 3**:** 135–143.

14. Feng B, Haas H, Marzluf GA (2000) ASD4, a new GATA factor of Neurospora crassa, displays sequence-specific DNA binding and functions in ascus and ascospore development. *Biochemistry* 39: 11065-11073.

15. Zhulin IB, Taylor BL, Dixon R (1997) PAS domain S-boxes in Archaea, Bacteria and sensors for oxygen and redox. *Trends Biochem Sci* 22: 331-333.

16. Haas H, Angermayr K, Stöffler G (1997) Molecular analysis of a *Penicillium chrysogenum* GATA factor encoding gene (sreP) exhibiting significant homology to the *Ustilago maydis* urbs1. *Gene* 184: 33-37.

17. Kumar PR, Yu Y, Sternglanz R, Johnston SA, Joshua-Tor L (2008) NADP regulates the yeast GAL induction system. *Science* 319: 1090-1092.

18. Finkel T, Deng CX, Mostoslavsky R (2009) Recent progress in the biology and physiology of sirtuins. *Nature* 460: 587 – 591.

19. Kankanala P, Czymmek K, Valent B (2007) Roles for Rice Membrane Dynamics and Plasmodesmata during Biotrophic Invasion by the Blast Fungus. *Plant cell* 19: 706 – 724.

20. Eastmond PJ, van Dijken AJ, Spielman M, Kerr A, Tissier AF, Dickinson HG, Jones JD, Smeekens SC, Graham IA (2002) Trehalose-6-phosphate synthase 1, which catalyses the first step in trehalose synthesis, is essential for Arabidopsis embryo maturation. *Plant J* 29: 225–235.

21. Sambrook J, Fritsch EF, Maniatis T (1989) Molecular Cloning: A laboratory manual. Cold Spring Harbor Laboratory Press, Cold Spring Harbor, N.Y.

22. Kershaw MJ, Talbot NJ (2009) Genome-wide functional analysis reveals that infection-associated fungal autophagy is necessary for rice blast disease. *Proc Natl Acad Sci U S A* 106: 15967-15972.

FIGURE LEGENDS

Fig 1. Tps1 controls G6PDH activity and binds NADPH. (*A*) Over-expression of the *G6PDH* gene under control of the β-tubulin gene promoter partially restores virulence to a Δ*tps1* mutant. Rice seedlings were inoculated with 1 x 10^4 spores ml^{-1}. (*B*). Tps1 binds NADPH. The intrinsic fluorescence of 2 μM NADPH was measured in solutions containing an increasing concentration of purified Tps1 protein. Excitation was at 340 nm, emission was measured at 465 nm. A decrease in fluorescence was observed with increasing Tps1 concentration consistent with removal of NADPH from solution by Tps1 protein binding. Assays were performed in triplicate. (*C*) Effect of NADPH fluorescence in the presence of TPS1 and G6P. Excitation was performed at 340 nm and the emission spectra recorded over wavelengths spanning 375 nm to 575 nm. Peak emission of NADPH fluorescence occurred at 465nm. The reaction mixture contained 1 μM Tps1, 15 μM NADPH, and 15 μM G6P, when present. NADPH alone provided the base-line level of the free solution state fluorescence. Addition of Tps1 quenched the fluorescence of NADPH. Addition of G6P caused an increase in fluorescence indicating that the NADPH is no longer bound and therefore no longer being quenched through the conformational fit of the ligand within the Tps1 binding site. (D) The homology structure of Tps1 reported in (4) was used to model interactions of the native substrates, G6P and UDP-glucose (left panel) and NADPH (right panel) with Tps1. NADPH can be modelled into the active site of Tps1, adopting a similar position within the binding site to that seen for UDP-glucose

and G6P. Calculated energies of binding for UDP-glucose (- 19 kcal/ mol), G6P (-19 kcal/ mol) and NADPH (-27 kcal/mol) suggest that NADPH binding to Tps1 is reversible and competitive.

Fig 2. Fungal virulence is controlled by Tps1 via the Nmr co-repessor proteins.

(*A*) Partial restoration of virulence to Δ*tps1*Δ*nmr1*, Δ*tps1*Δ*nmr2* and Δ*tps1*Δ*nmr3* double mutants of *M. oryzae*. Rice seedlings were inoculated with 1 x 10^{4} spores ml^{-1}. (*B*). Bar charts of lesion densities of Guy11, Δ*tps1*, Δ*tps1*Δ*nmr1*, Δ*tps1*Δ*nmr2* and Δ*tps1*Δ*nmr3* mutants. Results are the average of three independent replicates and error bars are the standard deviation. Bars with the same letter are not significantly different (Student's t-test, $P \leq 0.05$). (*C*) Low-stringency yeast two-hybrid analysis of physical interactions between Nut1, Nmr1, Nmr2, Nmr3 and Tps1 compared to the empty vector controls. –BD are strains carrying an empty *GAL4* DNA binding domain vector. –AD are strains carrying an empty *GAL4* activation domain vector. X-gal is supplemented in the media, and low stringency protein-protein interactions result in βgalactosidase gene expression and formation of blue colonies. (*D*) Rice infections were carried out with Δ*tps1*, Δ*tps1*Δ*nmr1*, Δ*tps1*Δ*nmr1:NMR1*, Δ*tps1*Δ*nmr1:NMR1*^{T13T} and Δ*tps1*Δ*nmr1:NMR1*^{T13V}. Expression of the *NMR1*^{T13V} allele does not complement the Δ*tps1*Δ*nmr1* mutant phenotype. Seedlings were inoculated with 1 x 10^{4} spores ml^{-1}.

Fig 3. qPCR analysis of *TPS1*-dependent gene expression. Genes encoding putative NADP(H)dependent enzymes (*NIA1, ALD1, KEF1, SDY1, OXD1 and OYE1*), known

virulence-associated genes (*MPG1* and *ALB1*), a putative metalloprotease (*MPT1*) and glucose-6-phosphate dehydrogenase (*G6PDH*) (for details see Table S1) were analyzed for expression. Strains were grown in CM for 48 h followed by 16 h growth in MM containing either 10 mM nitrate (closed bars) or 10 mM ammonium (open bars) as sole nitrogen source. Gene expression results were normalised against expression of the β-tubulin gene (*TUB2*). Results are the average of at least three independent replicates and error bars are the standard deviation. (*A*) Bar charts showing gene expression in Guy11, Δ*tps1* and Δ*nut1* mutant. *ALD1*, *KEF1*, *SDY1*, *OXD1* and *ALB1* are nitrate-inducible and dependent on the presence of *TPS1* and *NUT1*. Expression is relative to gene expression in the wild type grown on nitrate. (*B*) Bar charts showing gene expression in Guy11, Δ*tps1* and Δ*nut1* mutant. *MPT1*, *MPG1* and *OYE1* appear nitrate-inducible and *TPS1*dependent, but independent of *NUT1*. Expression is relative to gene expression in the wild type grown on nitrate. (*C*) Bar charts showing gene expression of all nine genes in conidia (black bar) and appressoria (grey bar) of Guy11. Expression is relative to *TUB2* gene expression. (*D*) Bar charts showing that *G6PDH* gene expression is partially restored in a Δ*tps1* mutant by

introduction of Δ*nmr1*, Δ*nmr2* or Δ*nmr3* gene deletions (*E*) Bar charts showing that *TPS1*dependent gene expression is partially restored in a Δ*tps1* mutant by introduction of Δ*nmr1*, Δ*nmr2* or Δ*nmr3* gene deletions. Expression is relative to gene expression in Δ*tps1* strains grown on nitrate.

Fig 4. A novel NADP(H)-dependent genetic switch is essential for fungal virulence in the rice blast fungus. (*A*) The Nmr repressors interact with three GATA transcription factors in *M. oryzae*. High stringency yeast two-hybrid analysis of physical interactions between Nut1, Asd4, Pas1, Sre1 and Nmr1, Nmr2, Nmr3 compared to empty vector controls. –BD are strains carrying an empty *GAL4* DNA-binding domain vector. –AD are strains carrying an empty *GAL4* activation domain vector. High stringency selection was on media lacking adenine, histidine, tryptophan and leucine. (*B*) Role of the GATA-factors Pas1 and Asd4 in pathogenicity. Δ*pas1* strains are fully pathogenic whereas Δ*asd4* strains are unable to infect host tissue. Rice seedlings were inoculated with 1×10^5 spores ml^{-1}. (*C*) A model for the action of Tps1 in virulence of *M. oryzae*. In response to G6P sensing, Tps1 activates G6PDH to produce NADPH from G6P and NADP in the oxidative pentose phosphate pathway. NADPH can bind to Tps1 to maintain a balance between G6P consumption and NADPH production. The conversion of NADP to NADPH inactivates the Nmr inhibitor proteins and results in the de-repression of genes encoding at least two known virulence factors, at least six NADPH-dependent proteins, and G6PDH. NADPH is subsequently consumed by NADPH-dependent proteins, such as NR. Under starvation conditions, such as found during appressorium formation on the surface of the leaf, the homeostatic balance between G6P consumption and NADPH production is not maintained, NADP levels are elevated, and the Nmr inhibitor proteins become activated leading to repression of the genes required for virulence. Proteins are indicated as black circles. TF = transcription factor (s). The corresponding genes are shown in red. UDP-glc is UDP-glucose.

Fig. 1 Tps1 controls G6PDH activity and binds NADPH.

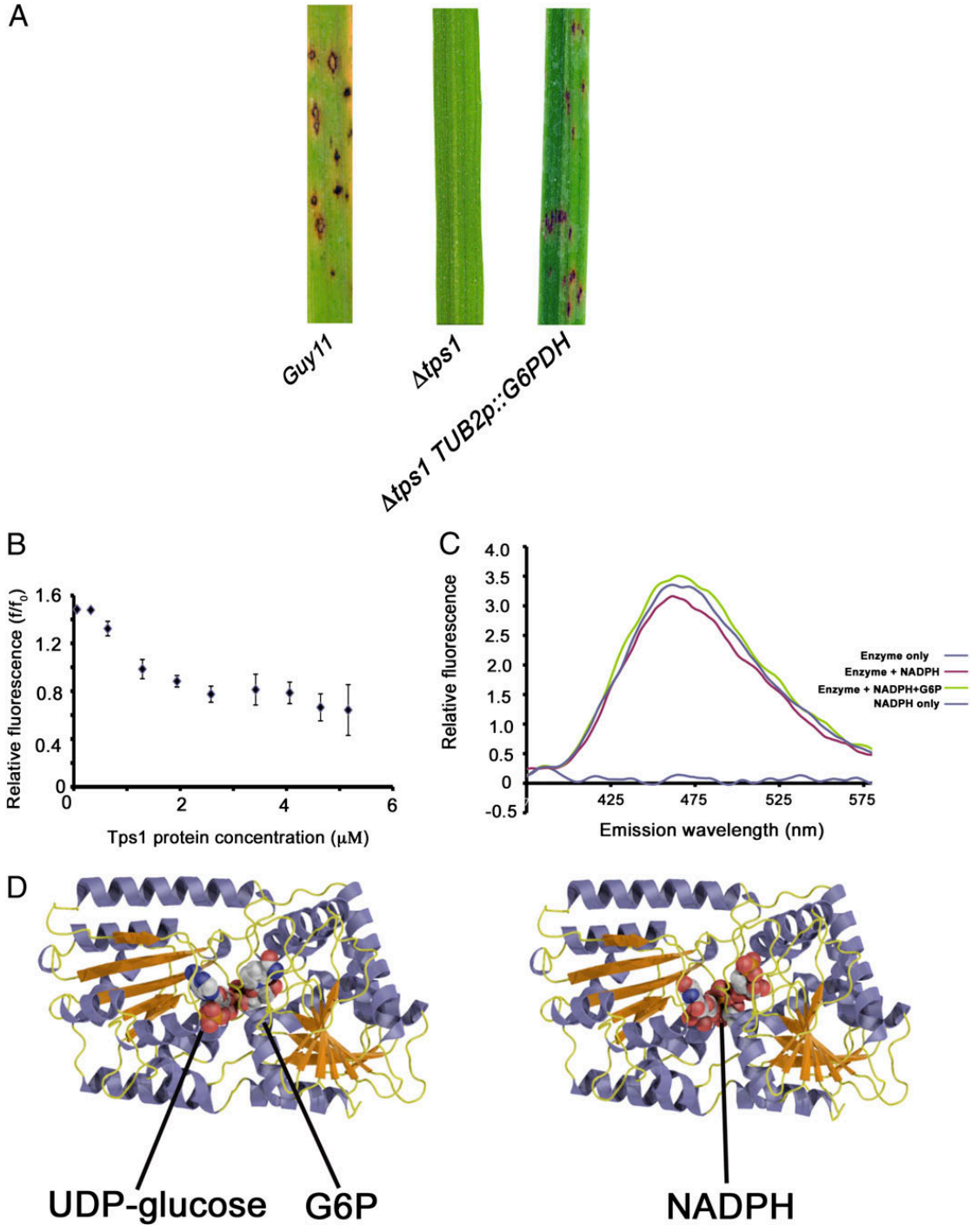

Fig. 2. Fungal virulence is controlled by Tps1 via the Nmr co-repessor proteins.

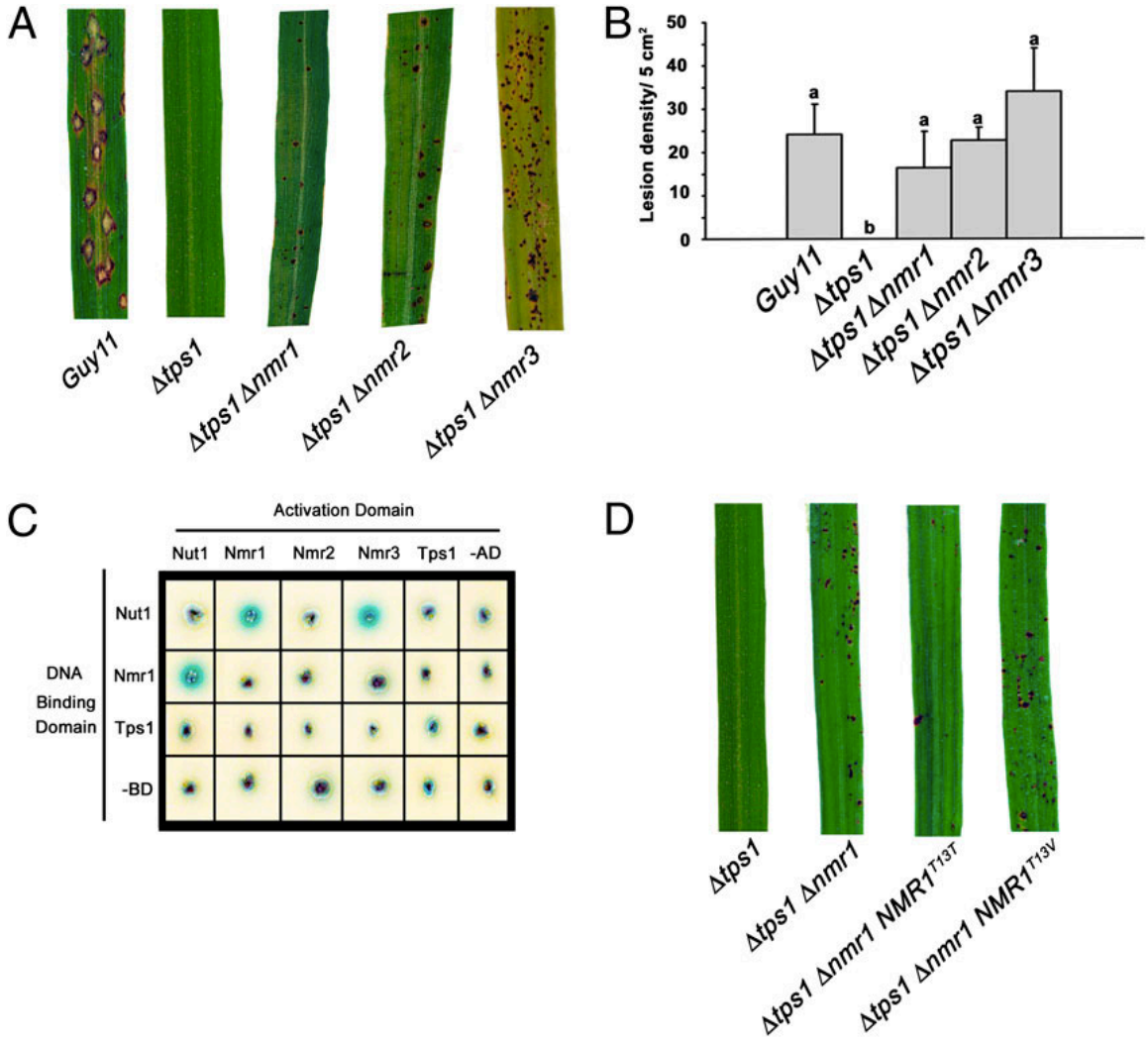

Fig 3. qPCR analysis of *TPS1*-dependent gene expression.

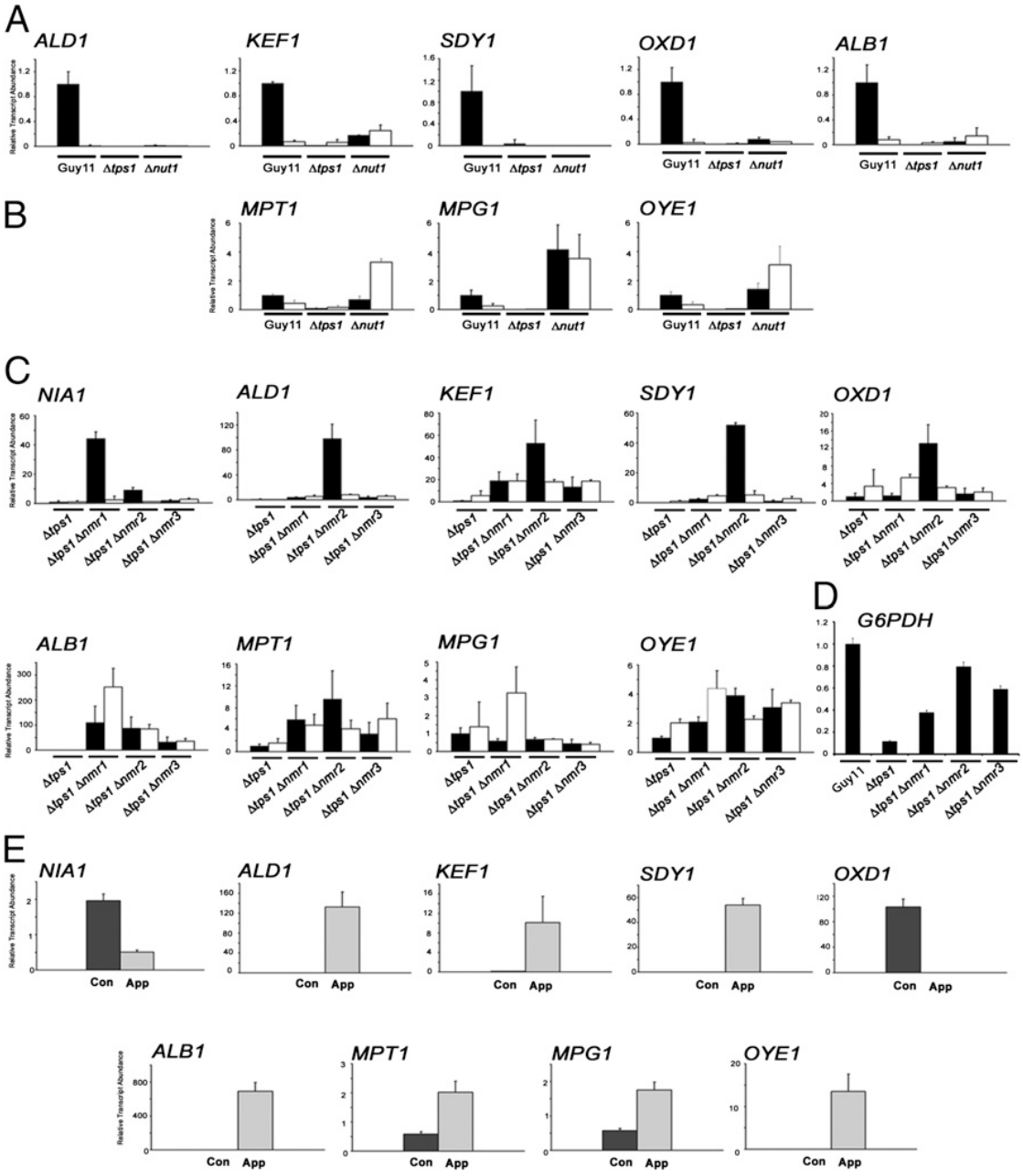

Fig 4. A novel NADP(H)-dependent genetic switch is essential for fungal virulence in the rice blast fungus.

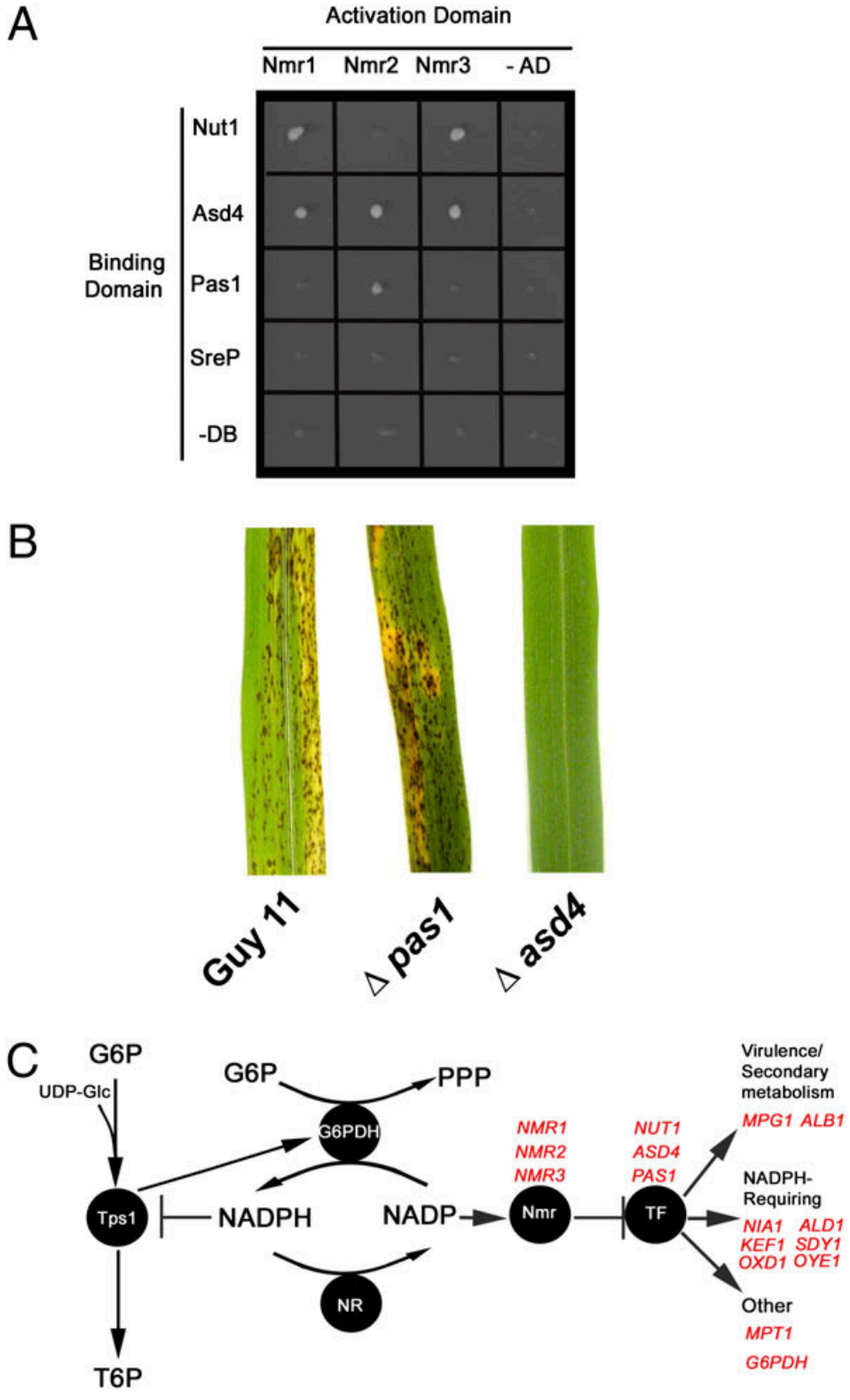

SUPPORTING INFORMATION

Supplementary Materials and Methods

Strains, physiological tests and plant infections

Strains were grown on complete medium (CM) containing 1 % (W/V) glucose, 0.2 % (W/V) peptone, 0.1 % (W/V) yeast extract and 0.1 % (W/V) casamino acids, or on glucose minimal medium (GMM) containing 10 % glucose and 0.6 % sodium nitrate, unless otherwise stated, as described in (1). For spore counts, 10 mm^2 blocks of mycelium were transferred to the centre of each plate, and the strains grown for 10 days at 26 ^oC. Colony diameters were measured, and the spores harvested in sterile distilled water, vortexed vigorously and counted on a haemocytometer (Corning). Spores were counted independently four times. Rice plant infections were made using a susceptible dwarf Indica rice (*Oryza sativa*) cultivar, CO-39 (2) as described previously (3). Fungal spores were isolated from 12 –14 day-old plate cultures and spray-inoculated onto rice plants of cultivar CO-39 in 0.2 % gelatin at a concentration of 5 x 10^4 spores / ml, unless otherwise stated, and disease symptoms allowed to develop for 96-144 hrs. Appressoria development was analyzed by inoculating a 240 µl droplet of water containing 1.5 X 10^4 spores onto plastic coverslips (Fisher) for development under hydrophobic conditions. Images were taken using a Nikon Eclipse 50i microscope and a Nikon DS-Fi1 Digital Sight camera. Infected leaves were imaged using an Epson Workforce scanner, and lesion sizes were determined based on pixel counts, following calibration of resolution, using ImageJ free software from NIH.

Enzyme assays

G6PDH activity was determined spectrophotometrically as described in (4).

QRT-PCR analysis

RNA was extracted from mycelium following the method of Timberlake (5). Strains were grown for 48 h in CM before switching to GMM for 16 hr. Mycelia was harvested, frozen in liquid nitrogen, and lyophilised overnight. cDNA synthesis was performed on 500 ng of DNase I (Invitrogen) treated RNA using the Affinityscript^{TM} QPCR synthesis kit (Stratagene). qRT-PCR was performed on an Mx3005P thermocycler (Stratagene) following the manufacturer's instructions. The qRT-PCR reaction was performed using 5 ng cDNA template and the Brilliant SYBR Green QPCR Master Mix (Stratagene). Thermocycler conditions were: 10 min at 95 ^{o}C, followed by 40 cycles of 95 ^{o}C for 30 sec, 63 ^{o}C for 30 sec and 72 ^{o}C for 30 sec. A final dissociation cycle was incorporated to ensure the specificity of each primer pair. Relative gene expression was calculated in Microsoft Excel from the determined Ct (dR) values. qRT-PCR primer pairs (Table S2) were designed following Stratagene's recommendations and using NetPrimer (Premier Biosoft).

Targeted gene replacement

Targeted gene replacement of the *M. oryzae ASD4*, *PAS1*, *NIA1*, *NUT1*, *NIR1*, *NMR1*, *NMR2* and *NMR3* genes, using the split marker strategy (6), is shown in Figure S6. All gene replacements were achieved by replacing 1 Kb of the gene of interest with the sulphonylurea resistance selectable marker, *ILV1* (2.8 Kb) (7), except Δ*nmr1* Δ*nmr2* double gene deletion strains where *NMR1* was replaced with the hygromycinB resistance

selectable marker, *hph* (1.7 Kb) (8), and Δ*nmr1* Δ*nmr2* Δ*nmr3* triple gene deletion strains where *NMR3* was replaced with the bialaphos resistance selectable marker, *bar* (0.9 Kb) (9). The two overlapping halves of the *ILV1* gene were amplified from pCB1532 (7) using M13F:IL and ILSplit, and M13R:LV1 and LV1Split (Table S2 and Fig. S6). M13F:IL introduces the M13F sequence to the 5' end of the *ILV1* gene, and M13R:LV1 introduces the M13R sequence to the 3' end of the *ILV1* gene. Similarly, the *bar* gene was amplified from pCB1530 (7) using M13F:ba and BaSplit, and M13R:ar and ArSplit, while the *hph* gene was cloned into pBluescript (Stratagene) as a 1.4 kb EcoRI - Xba I fragment and the two halves amplified using M13F and HYSplit, and M13R and YGSplit. The sequence of genes to be disrupted by targeted gene replacement were retrieved from the *M. oryzae* genome database at the Broad Institute (Massachusetts Institute of Technology, Cambridge, MA) (www.broad.mit.edu/annotation/fungi/magnaporthe) and used to design specific primers (Table S2). First and second round PCR amplification used the following thermocycler conditions: 1 min at 95 ^{o}C followed by 35 cycles of 30 sec at 95 ^{o}C, 30 sec at 63 ^{o}C and 3 min at 68 ^{o}C. The PCR reaction was performed using *pfu* taq (Promega) and each amplified product was purified using a PCR purification kit (Promega). The *M. oryzae* Guy11 strain or Δ*tps1* was transformed with each deletion cassette (5 µg of DNA of each flank). Transformants were selected in the presence of chlorimuron ethyl (100 µg mL-1) for sulphonylurea resistance, BASTA (100 µg mL-1) for bialaphos resistance and hygromycin B (200 µg mL-1) for hygromycin resistance. Gene replacement was

confirmed by PCR and qRT-PCR. At least two independent deletion mutants from each targeted gene replacement were studied to confirm the mutant phenotype.

Gene fusion and mutagenic constructs

The split marker method described above was adapted to create constructs for protein function analysis (Table S2). A gene fusion construct carrying *G6PDH* fused to the *β-tub1p* promoter sequence was created by first amplifying a 1 Kb DNA fragment, including the promoter, upstream of the β-tubulin gene using b-tubF and b-tubG6R, and the *G6PDH* gene, from the translation start site and including the 3' UTR, using b-tubG6F and OEG6R1. This generated a 1Kb upstream region of *TUB2*, including the promoter, with a 22 bp overhang at the 3' end encoding the 5' end of *G6PDH*, and a 2.6 Kb fragment, encoding the *G6PDH* gene, with a 22 bp overhang at the 5' end encoding the 3' end of the *TUB2* promoter. In the second round, these two fragments were amplified together in a PCR reaction using nested 5' (b-tub nes F) and nested 3' (NesOEG6R) primers that also carried sequences for the *Not*I restriction site (underlined in Table S2). The resulting PCR product was purified and subcloned into pGEM-T (Promega), digested out of pGEM-T as a 3.6 Kb *Not*I-*Not*I fragment, and subcloned into the *Not*I site of pCB1530 (7) to give pOEG6PDH-BASTA. Δ*tps1* strains were transformed with this vector and transformants selected on BASTA (100 μg mL-1).

A mutation was introduced into the coding region of *NMR1*, to encode the amino acid change T13V, as follows. A 1 Kb upstream fragment of *NMR1*, including the first 39 bp of the gene, was amplified using T13VF1 and T13VR1 to introduce the nucleotide change ACC to GCC (encoding T13V) at the 3' end of the PCR fragment. The *NMR1*

gene, and the 3' UTR, was amplified by T14VF2 and T13VR2 to give a 1.6 Kb fragment carrying the nucleotide change ACC to GCC at the 5' end of the PCR product. These two products were amplified together in the second round PCR reaction using the nested primers T13VnesF and T13VnesR. These primers also carried sequences for the *Not*I restriction site (underlined in Table S2). The resulting PCR product was purified and subcloned into pGEM-T (Promega), digested out of pGEM-T as a 2.7 Kb *Not*I-*Not*I fragment, and subcloned into the *Not*I site of pCB1530 (7) to give pNMR1-T13V. A control plasmid was constructed by amplifying the *NMR1* gene with T13VnesF and T13VnesR and subcloning first into pGEM-T and then into the *Not*I site of pCB1530 (as described above) to give pNMR1-T13T. Δ*tps1* strains were transformed with these vectors and transformants selected on BASTA (100 µg mL-1).

In all cases, PCR conditions were as described for the split marker gene replacement strategy above.

Yeast two-hybrid construction

Protein-protein interactions were analysed using the Matchmaker^{TM} GAL4 Two-Hybrid System 3 kit from Clontech. cDNA synthesised from RNA using the Affinityscript^{TM} QPCR synthesis kit (Stratagene) described above was used as a template in a PCR reaction with gene specific primers designed to incorporate endonuclease restriction sites at each end of the PCR product (Table S2, restriction sites underlined and included in the primer name). The thermocycler reaction conditions were 1 min at 95 ^{o}C followed by 35 cycles of 30 sec at 95 ^{o}C, 30 sec at 63 ^{o}C and 3 min at 68 ^{o}C. The PCR reaction was performed using *pfu* taq (Promega) and each amplified product was purified using a PCR

purification kit (Promega). The PCR product, encoding the protein of interest from start site to termination codon, was subcloned into pGEM-T (Promega). The product was then digested out of pGEM-T using the restriction sites included on either primer, and subcloned, in frame, into the multicloning site of pGBKT7 and/ or pGADT7. pGBKT7 carries sequences encoding the GAL4 DNA-binding domain and pGADT7 carries sequences encoding the GAL4 activation domain. The resulting *GAL4* gene fusion vectors were transformed into yeast strain AH109 following Clontech's Yeast Protocols handbook. AH109 has the genotype *MATa, trp1-901, leu2-3, 112, ura3-52, his3-200, gal4Δ, gal80Δ, LYS2::GAL1*$_{UAS}$*-GAL1*$_{TATA}$*-HIS3, GAL2*$_{UAS}$*-GAL2*$_{TATA}$*-ADE2, URA3::MEL1*$_{UAS}$*-MEL1*$_{TATA}$*-lacZ* (10) and is unable to grow on minimal media lacking adenine, histidine, leucine and tryptophan. pGBKT7 confers tryptophan prototrophy to AH109, and pGADT7 confers leucine prototrophy to AH109. In addition, AH109 strains carrying *GAL4* gene fusion constructs encoding proteins that interact are also able to grow on media lacking adenine and histidine because the genes for adenine and histidine prototrophy are fused to the Gal promoter. Therefore, protein-protein interactions were identified in our study using the most stringent selection screen of growth of AH109 strains on adenine, histidine, leucine and tryptophan (Fig 4*A*). In addition, we also used a low stringency selection to screen for weak interactions between our proteins of interest. AH109 strains also carry the ß-galactosidase-encoding gene fused to the Gal promoter. In a low stringency protein interaction screen, X-gal (5-bromo-4-chloro-3-indolyl- beta-D-galactopyranoside) was added to minimal media lacking tryptophan and leucine only. All colonies carrying pGBKT7 and pGADT7 could grow on this media, and interactions

between proteins encoded on these vectors were observed by the appearance of blue colonies (Fig 2*C*). High- and low stringency selections were performed following the manufacture's protocols.

Tps1 protein overexpression and purification

M. oryzae cDNA, synthesized as described above, was used as a template to amplify the *TPS1* coding sequence using Platinum Pfx polymerase (Invitrogen) and the oligonucleotides 5' BamHI-Tps1 (I) and 3' EcoRI-Tps1, introducing the BamHI and EcoRI restriction endonuclease sites at the 5' and 3' termini. The 1.6 Kb product was ligated into the cloning vector pCR-Blunt (Invitrogen) and subcloned into the pMBPTEV expression vector, a pET28b (Novagen) derivative containing the DNA sequence of the maltose binding protein (MBP) and TEV protease recognition site (11) from the plasmid pRK1043 (Addgene plasmid 8835). The oligonucleotides 5' ndeI-Tps1 and 3' BamHI-Tps1 (II) introduced the NdeI and BamHI restriction endonuclease sites required for in-frame cloning of the fusion protein. The MBP-tev fusion was ligated in the previously stated cloning vector prior to the expression vector. The pMBPTEV and the Tps1 fusion protein construct, pMBPTEV-TPS1, were propagated through *Escherichia coli* Top10 cells (Invitrogen). Production of the soluble fusion protein required expression within the *ArcticExpress*™ (DE3) RIL strain (Stratagene). Liquid cultures were grown at 37 ^{o}C, 225rpm in LB supplimented with kanamycin (30ug / mL). Once an OD600nm of approximatley 0.8 was reached, the cultures were cooled to 12 ^{o}C for 45 minutes and then

1 mM isopropyl-thio-[beta]-D-galactoside (IPTG) was added to induce overexpression. The cells were harvested by centrifugation after a further 24 hours of growth and resuspended in 25mM TrisHCl pH8, 300mM NaCl and 1mM DTT. Complete lysis was achieved by one round of freeze-thawing, and sonication within an ice-water bath with cellular debris removed by centrifugation at 18000g, 10 ^{oC} for 30 mins. The supernatant was loaded onto a 5 mL MBPTrap HP (GE Healthcare) column pre-equilibrated with the sonciation buffer. Unbound proteins were removed by washing 10 CV of sonication buffer through the column and the Tps1-fusion protein collected by 10 CV of sonication buffer supplemented with 10 mM maltose. The Tps1-fusion solution was buffer exchanged and concentrated to 1/10th the original volume in 20mM TrisHCl pH8, 150mM and 1mM DTT using an Amicon (Millipore) stirred cell with a 30 kDa NMWL ultrafiltration membrane under 45psi nitrogen at room temperature. The protein solution was loaded onto a HiLoad16/60 Superdex 200 gel-filtration column (GE Healthcare) pre-equilibrated with the same buffer and purified to homogeneity.

Measurement of NADPH binding by purified Tps1 fusion protein

The intrinsic fluorescence of NADPH (12, 13, 14, 15) was measured at 25 ^{o}C using a Cary Eclipse Fluorescence spectrophotometer (Varian). Fresh solutions of TPS1, NADPH and G6P were prepared daily in 10 mM TrisHCl pH 8.0 and equilibrated until a constant fluorescence spectrum was achieved. Bound NADPH to TPS1 using the substrate fluorescence was excited at 340 nm (5nm-slit width) and the emission spectra recorded from 360 nm – 550 nm (10 nm-slit width). Intrinsic tryptophan fluorescence at

an excitation at 295 nm (5nm-slit width) produced an emission spectra from 320nm-550nm (5nm-slit width). All data was corrected for dilution and background scattering.

Titration of NADPH to TPS1 was used to determine specific binding. A 1μM TPS1 solution as described above was titrated with NADPH. The binding event was monitored by tryptophan fluorescence quenching at 340 nm after excitation at 295 nm. Each spectrum was corrected for unbound NADPH in solution. Internal filtering effects were negligible at the experiment concentrations of TPS1 and NADPH. Data from the titration was fitting by nonlinear regression using Origin 8 (OriginLab, Northampton, MA). A one-site binding curve described by the Hill equation best fit the data.

Computational docking

The Molecular Operating Environment package, MOE 2008.10 (Chemical Computing Group Inc., Montreal, Canada) was used to assess ligand binding within Tps1. The previously reported Tps1 homology structure (4) was used to calculate the conformationally energy minimised docking for NADPH, UDP-glucose and glucose-6-phosphate. The ligand structures were protonated (300K, pH 7 and 0.1M salt) and MMFF94 forcefield atomic charges assigned and minimised using the default settings prior to docking. The protein structure was also subjected to the same protonation and forcefield assignment but no further energy minimisation was performed on the homology model structure to prevent computationally introduced artefacts. The active site was defined as 6Å surrounding the position of the native ligands within the model structure. The native ligands were docked to assess the computed free energy of the system with regards the NADPH docking. Glucose-6-phosphate was docked in the

presence of UDP-glucose as previous crystallographic evidence suggests the sugar-nucleotide donor must be present for the acceptor to bind (16). The initial docking round used the Triangle Matcher placement methodology and the London dG scoring function. The top 50 unique placements were retained and a forcefield parameterisation refinement imposed and rescored as previously stated. The remaining 30 unique ligand conformations were assessed with respect to the overall calculated scoring function (kcal / mol).

Supplementary References

1. Foster AJ, Jenkinson JM Talbot NJ(2003) Trehalose synthesis and metabolism are required at different stages of plant infection by *Magnaporthe grisea*. *EMBO J* 22: 225-235.

2. Valent B, Farrall L, Chumley FG (1991) *Magnaporthe grisea* genes for pathogenicity and virulence identified through a series of backcrosses. *Genetics* 127: 87-101.

3. Talbot NJ, Ebbole DJ, Hamer JE (1993) Identification and characterization of MPG1, a gene involved in pathogenicity from the rice blast fungus *Magnaporthe grisea*. *Plant Cell* 5: 1575-1590.

4. Wilson RA, Jenkinson, JM, Gibson, RP, Littlechild, JA, Wang, ZY, Talbot, NJ (2007)

Tps1 regulates the pentose phosphate pathway, nitrogen metabolism and fungal virulence.
EMBO J 26: 3673-3685.

5. Timberlake WE (1980) Developmental gene regulation in *Aspergillus nidulans*. *Dev Biol* **78:** 497–510.

6. Catlett NL, Lee B-N, Yoder OC, Turgeon BG (2003) Split-Marker Recombination for Efficient Targeted Deletion of Fungal Genes. *Fungal Genet Newsl* 50: 9-11.

7. Sweigard J, Chumley FG, Carroll A, Farrall L, Valent B (1997) A series of vectors for fungal transformation. *Fungal Genet Newsl* 44: 52-53.

8. Carroll AM, Sweigard JA, Valent B (1994) Improved vectors for selecting resistance to hygromycin. *Fungal Genet Newsl* 41: 22.

9. Pall ML, Brunelli JP (1993) A series of six compact fungal transformation vectors containing polylinkers with multiple unique restriction sites. *Fungal Genet Newsl* 40: 59-63.

10. James P, Haliaday J, Craig EA (1996) Use of the two-hybrid system to identify the domain of p53 involved in oligomerization. *Oncogene* 8: 1693 – 1696.

11. Kapust RB, Tözsér J, Fox JD, Anderson DE, Cherry S, Copeland TD, Waugh DS (2001) Tobacco etch virus protease: mechanism of autolysis and rational design of stable mutants with wild-type catalytic proficiency. *Protein Eng* 14: 993 – 1000.

12. McDonald G, Brown B, Hollis D, Walter C (1972) Some effects of environment on the folding of nicotinamide-adenine dinucleotides in aqueous solutions. *Biochemistry* 11: 1920-1930.

13. Hull RV, Conger PS, Hoobler RJ (2001) Conformation of NADH studied by fluorescence excitation transfer spectroscopy. *Biophys Chem* 90: 9 – 16.

14. Li, B and Lin, S-X (1996) Fluorescence-energy transfer in human estradiol 17ß-dehydrogenase-NADPH complex and studies on the coenzyme binding. *Eur. J. Biochem* 235: 180-186.

15. Fruscione, F, Sturla, L, Duncan, G , Van Etten, JL, Valbuzzi, P., De Flora, A. , Di Zanni, E. and Tonetti, M. (2008) Differential Role of NADP+ and NADPH in the activity and structure of GDP-D-mannose-4,6-dehydratase from two Chlorella viruses. *J. Biol. Chem.* 283: 184-193.

16. Gibson RP, Turkenburg JP, Charnock SJ, Lloyd R, Davies GJ (2002) Insights into trehalose synthesis provided by the structure of the retaining glucosyltransferase OtsA. *Chem Biol* 9: 1270-1273.

Supplementary Figures

Fig S1. Targeted deletion of genes required for nitrate metabolism do not affect the ability of the fungus to cause disease. However, as previously described (1), nitrate utilizing mutants have reduced lesion sizes compared to Guy11. Strains were inoculated onto rice at a rate of 5 X 10^4 spores ml $^{-1}$.

1. Froeliger, E. H., Carpenter, B.E. NUT1, a major nitrogen regulatory gene in *Magnaporthe grisea*, is dispensable for pathogenicity. Mol. Gen. Genet. 251, 647-656 (1996).

Fig S2. *G6PDH* and *TUB2* gene transcript analysis. (*A*) *G6PDH* gene expression in Δ*tps1* compared to Guy11. Strains were grown in complete media (CM) for 48 h followed by 16 h growth in nitrate. Gene expression results were normalised against *TUB2* expression and are given relative to gene expression in Guy11 on nitrate. Results are the average of at least three independent replicates and error bars are standard deviation. (*B*) *G6PDH* gene expression in Guy11 appressoria (closed bars) compared to conidia (open bars). Gene expression results were normalised against *TUB2* expression. Results are the average of at least three independent replicates and error bars are standard deviation. (*B*) Comparison between *TUB2* and *G6PDH* gene expression in Δ*tps1* strains grown in CM for 48 h followed by 16 h growth in nitrate. Results are the average of at least three independent replicates and error bars are standard deviation.

Fig S3. Analysis of NADPH binding by Tps1. (*A*) NADPH titration against Tps1. Changes to the intrinsic fluorescence of tryptophan in TPS1 was measured. Excitation was performed at 295 nm, and emission was monitored at 340 nm and corrected for NADPH absorption and dilution. The addition of NADPH causes a quenching of trp fluorescence. The Hill Equation describes the binding of a ligand to a macromolecule and whether the binding is enhanced when other ligand molecules are already present (i.e. cooperative binding). To calculate the Hill coefficient, the corrected change in emission fluorescence (ΔF) was plotted against the concentration of NADPH (L) to calculate the dissociation constant (KD). The obtained fluorescence data was analysed by non-linear regression of the one-site binding equation using the Origin 8.1 program (OriginLab, Northampton, MA), where:

$\Delta F = (\Delta Fmax \times Lh) / (KD + Lh)$

ΔF is the change in fluorescence, ΔFmax is the maximum change in fluorescence, L is the ligand concentration and h is the Hill slope. (*B*) Effect of NADPH fluorescence in the presence of TPS1 and G6P Excitation was performed at 340 nm and the emission spectra recorded over wavelengths spanning 375 nm to 575 nm. Peak emission of NADPH fluorescence occurred at 465nm. The reaction mixture contained 1 mM Tps1, 15 mM NADPH, and 15 mM G6P, when present. The enzyme alone did not contribute to the overall 465nm emission. NADPH alone provided the base-line level of the free solution state fluorescence. TPS1 with NADPH produces a quenched fluorescence of the NADPH signal (as observed in Figure 1). Addition of G6P produces an increase in the

fluorescence of the system indicating that the NADPH is no longer bound and therefore no longer being quenched through the conformational fit of the ligand within the TPS1 binding site.

Fig S4. Functional characterization of the Nmr co-repressor complex. (*A*) Top panel; qPCR analysis of gene expression from Guy11, *Δtps1* and Δ*nut1* strains grown in CM for 48 h followed by 16 h growth in minimal media containing either 10 mM nitrate (closed bars) or 10 mM ammonium (open bars) as sole nitrogen source. *MEP1* and *MEP2* are two genes with homology to ammonium transporters from yeast (Tabe S1). Δ*tps1* strains express these transporter genes even in the absence of ammonium. Gene expression results were normalised against *TUB2* expression and compared relative to the expression of each gene in Guy11 strains grown on nitrate. Results are the average of at least three independent replicates and error bars are standard deviation. Bottom panel; a proposed schematic of gene regulation in response to nitrate (NO_3^-) during vegetative growth. In the absence of Tps1, Nmr1 is constitutively present and bound to Nut1, preventing *NIA1* gene expression and causing the fungus to adopt an ammonium-responsive status irrespective of nitrogen source. Arrows indicate activation, cross bars indicate inhibition. (*B*) Three homologues of the *A. nidulans nmrA* gene are present in the *M. oryzae* genome and encode Nmr1, Nmr2 and Nmr3. Regions of identity between the NMRA, Nmr1, Nmr2 and Nmr3 proteins are highlighted. Black asterisks beneath amino acids indicate those residues determined in NMRA to be involved in binding NADP. Red asterisk indicates residue Thr-14 of NMRA and Thr-13 of Nmr1, Nmr2 and Nmr3. (*C*) Targeted gene deletion of *NMR1*, *NMR2* and *NMR3* in GUY11 do not affect pathogenicity and

result in strains that are fully virulent. Strains were inoculated at a rate of 1 X 10^5 spores ml $^{-1}$. (*D*) Nitrate reductase activity of Guy11 strains grown in CM for 48 h then switched to growth on GMM with 10 mM ammonium as nitrogen source for 16 h was determined following Wilson et al (1). Activity is given as a percentage of Guy11 nitrate reductase activity following growth for 16 h on nitrate-containing media. In *A. nidulans*, deletion of *nmrA* results in constitutive activation of AREA resulting in inappropriate nitrate reductase activity during growth on ammonium (2). However, in *M. oryzae*, nitrate reductase activity was only detected during growth on ammonium for strains carrying two or more *NMR* gene deletions in the Guy11 background, suggesting that the interaction between Nut1 and the Nmr proteins is more complex in *M. oryzae*. In addition, the detection of nitrate reductase activity in the Δ*nmr1* Δ*nmr2* double mutant strains compared to either single parent strains provides evidence that Nmr2 interacts at least indirectly with Nut1 *in vivo*, accounting for the inability to detect any direct interaction between these two proteins in the yeast two-hybrid screen (Fig. 2*C*). *(E)* Nitrate reductase activity is partially remediated in the Δ*tps1Δnmr1* and Δ*tps1Δnmr2* suppressor strains. Nitrate reductase activity was determined as described in (1) for strains switched to growth in GMM with nitrate (closed bars) or ammonium (open bars) as nitrogen source. Enzyme activity is given as a percentage of Guy11 nitrate reductase activity during growth on nitrate. Results are the average of at least three independent replicates and error bars are standard deviation. (*F*) Sporulation of Δ*tps1* suppressor strains is partially remediated in some suppressor strains when grown on nitrate-containing media compared to the Δ*tps1* parental strains. Results are the average of at

least three independent replicates and error bars are standard deviation. Bars with the same letter are not significantly different (*student's t-test*, $p \leq 0.05$).

1. Wilson RA, Jenkinson, JM, Gibson, RP, Littlechild, JA, Wang, ZY, Talbot, NJ (2007) Tps1 regulates the pentose phosphate pathway, nitrogen metabolism and fungal virulence. *EMBO J* 26: 3673-3685.

2. Andrianopoulos A, Kourambas S, Sharp JA, Davis MA, Hynes MJ (1998) Characterization of the Aspergillus nidulans *nmrA* Gene Involved in Nitrogen Metabolite Repression. *J Bacteriol* 180: 1973–1977.

Fig S5. Physiological analysis of Δ*pas1* and *Δasd4* strains. (*A*) Δ*asd4* strains are reduced in radial growth compared to Δ*pas1* and Guy11 strains. Strains were grown on complete media for 10 days. (*B*) Δ*pas1* and Δ*asd4* strains are altered in sporulation during growth on nitrate and ammonium minimal medium. Spores were harvested from 10 day old cultures. Bars are the average of four independent replicates. Bars with the same letter are not significantly different ($p \leq 0.05$). (*C*) Appressorium development is abolished in Δ*asd4* strains compared to Guy11. Appressoria were induced on plastic cover slips and analyzed after 2, 8 and 36 hrs.

Fig S6. shows the split marker strategy employed to construct gene replacement vectors. In this example, *ILV1,* conferring resistance to sulphonylurea, is shown. In the first round of PCR, 1 Kb of sequence upstream of the gene of interest, the left flank (LF), is amplified from genomic DNA using LF5' and LF3', with LF3' introducing M13F

sequences to the 3’ end of the PCR product. 1 Kb of sequence downstream of the gene of interest, the right flank (RF), is amplified from genomic DNA using RF5’ and RF3’, with RF5’ introducing M13F sequences to the 5’ end of the PCR product. The two overlapping halves of *ILV1* are amplified from pCB1532 using M13F:IL and ILSplit, and M13R:LV1 and LV1Split, to generate M13F sequences at the 5’ of the IL fragment, and M13R sequences at the 3’ of the LV1 fragment. In the second round of PCR, LF is amplified with IL in a PCR reaction using a nested LF primer (NesF) and ILSplit to generate LF fused to the 5’ half of *ILV1*, while RF is amplified with LV1 in a PCR reaction using a nested RF primer (NesR) and LV1Split to generate RF fused to the 3’ half of *ILV1*. These two fragments were purified and co-transformed into Guy11. Transformants were rapidly screened for gene replacement using the outer LF5’ and RF3’ primers.

Fig. S1

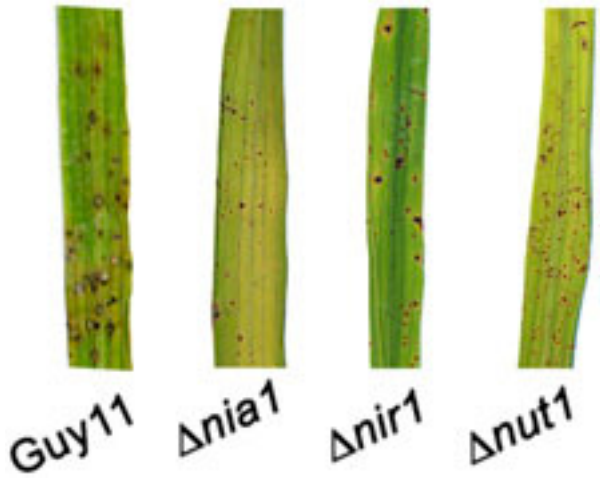
Guy11
Δnia1
Δnir1
Δnut1

Fig. S2

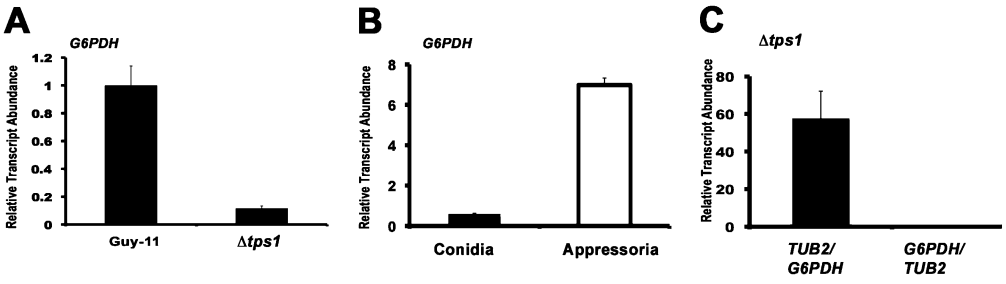
A
G6PDH
Relative Transcript Abundance
1.2
1
0.8
0.6
0.4
0.2
0
Guy-11
Δtps1
B
G6PDH
Relative Transcript Abundance
8
6
4
2
0
Conidia
Appressoria
C
Δtps1
Relative Transcript Abundance
80
60
40
20
0
TUB2/ G6PDH
G6PDH/ TUB2

Fig. S3

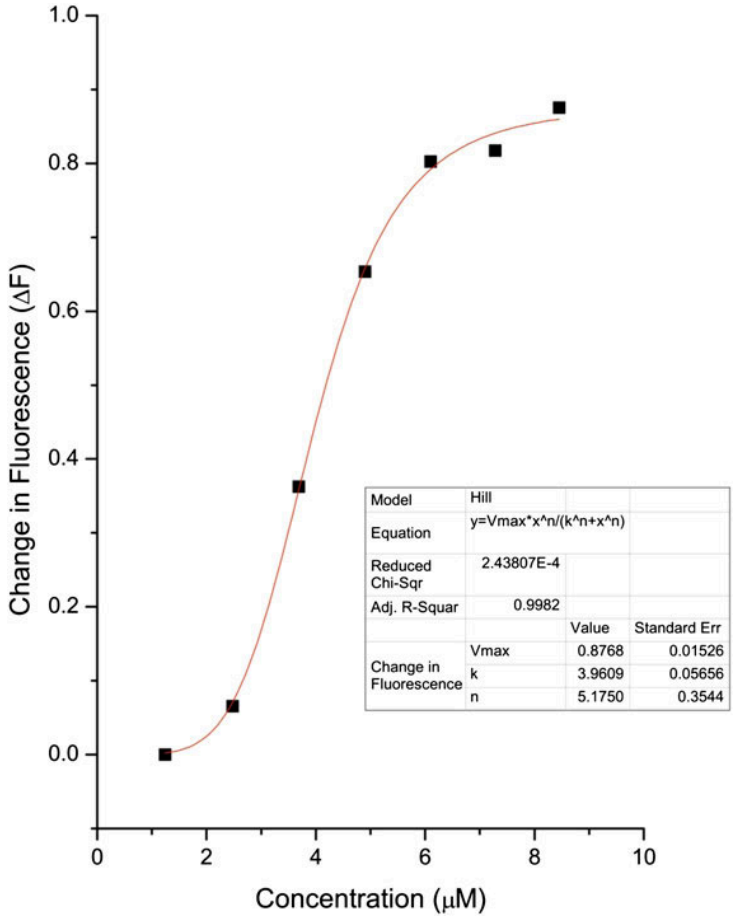
Change in Fluorescence (ΔF)
Concentration (μM)
1.0
0.8
0.6
0.4
0.2
0.0
0
2
4
6
8
10
Model Hill
Equation y=Vmax*x^n/(k^n+x^n)
Reduced Chi-Sqr 2.43807E-4
Adj. R-Squar 0.9982
Value Standard Err
Change in Fluorescence Vmax 0.8768 0.01526
k 3.9609 0.05656
n 5.1750 0.3544

Fig. S4

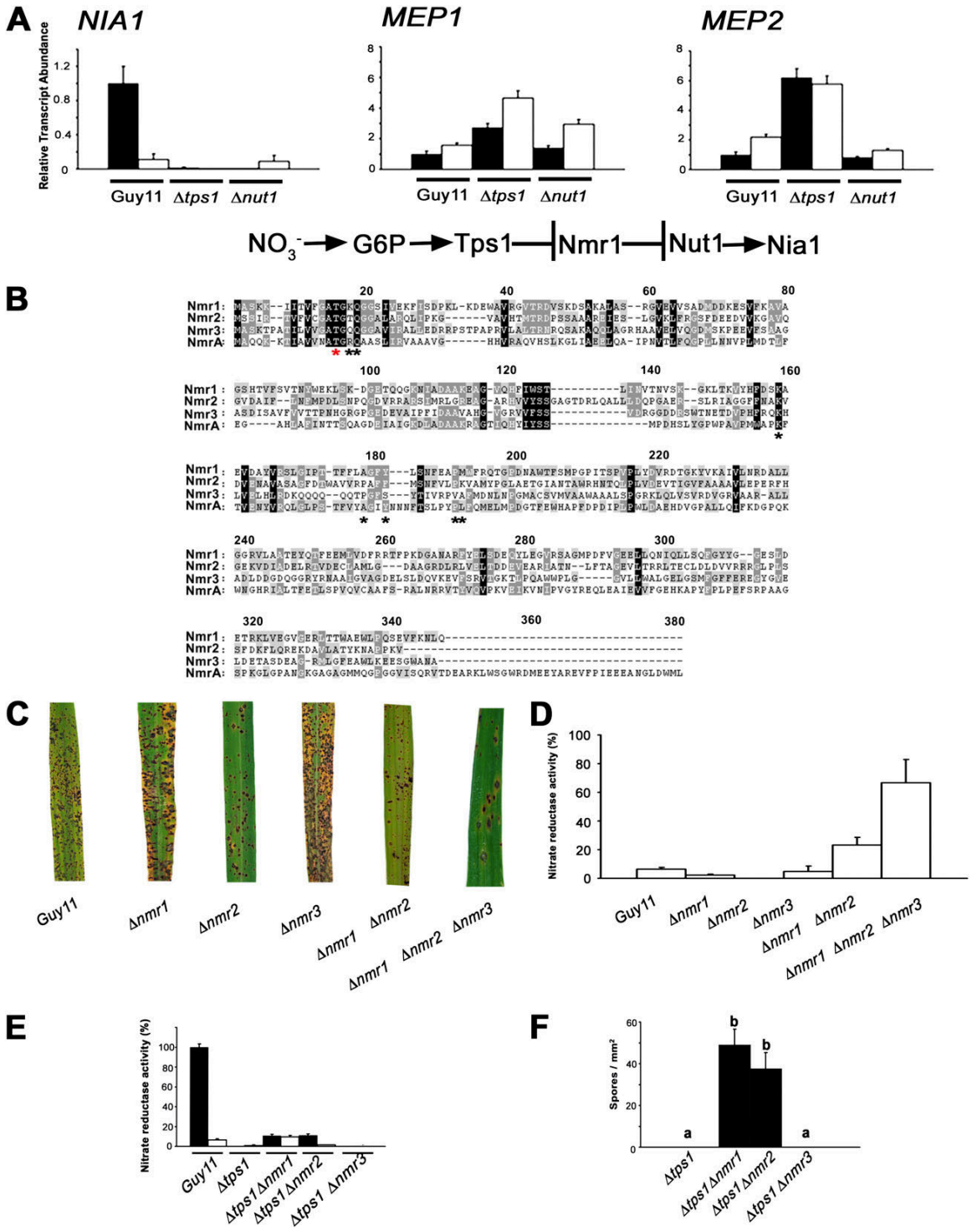
A
NIA1
MEP1
MEP2
Relative Transcript Abundance
Guy11
Δtps1
Δnut1
NO3- → G6P → Tps1 ⊣ Nmr1 ⊣ Nut1 → Nia1
B
Nmr1
Nmr2
Nmr3
NmrA
C
Guy11
Δnmr1
Δnmr2
Δnmr3
Δnmr1 Δnmr2
Δnmr1 Δnmr2 Δnmr3
D
Nitrate reductase activity (%)
E
Nitrate reductase activity (%)
Guy11
Δtps1
Δtps1Δnmr1
Δtps1Δnmr2
Δtps1 Δnmr3
F
Spores / mm²
a
b
b
a
Δtps1
Δtps1Δnmr1
Δtps1Δnmr2
Δtps1Δnmr3

Fig. S5

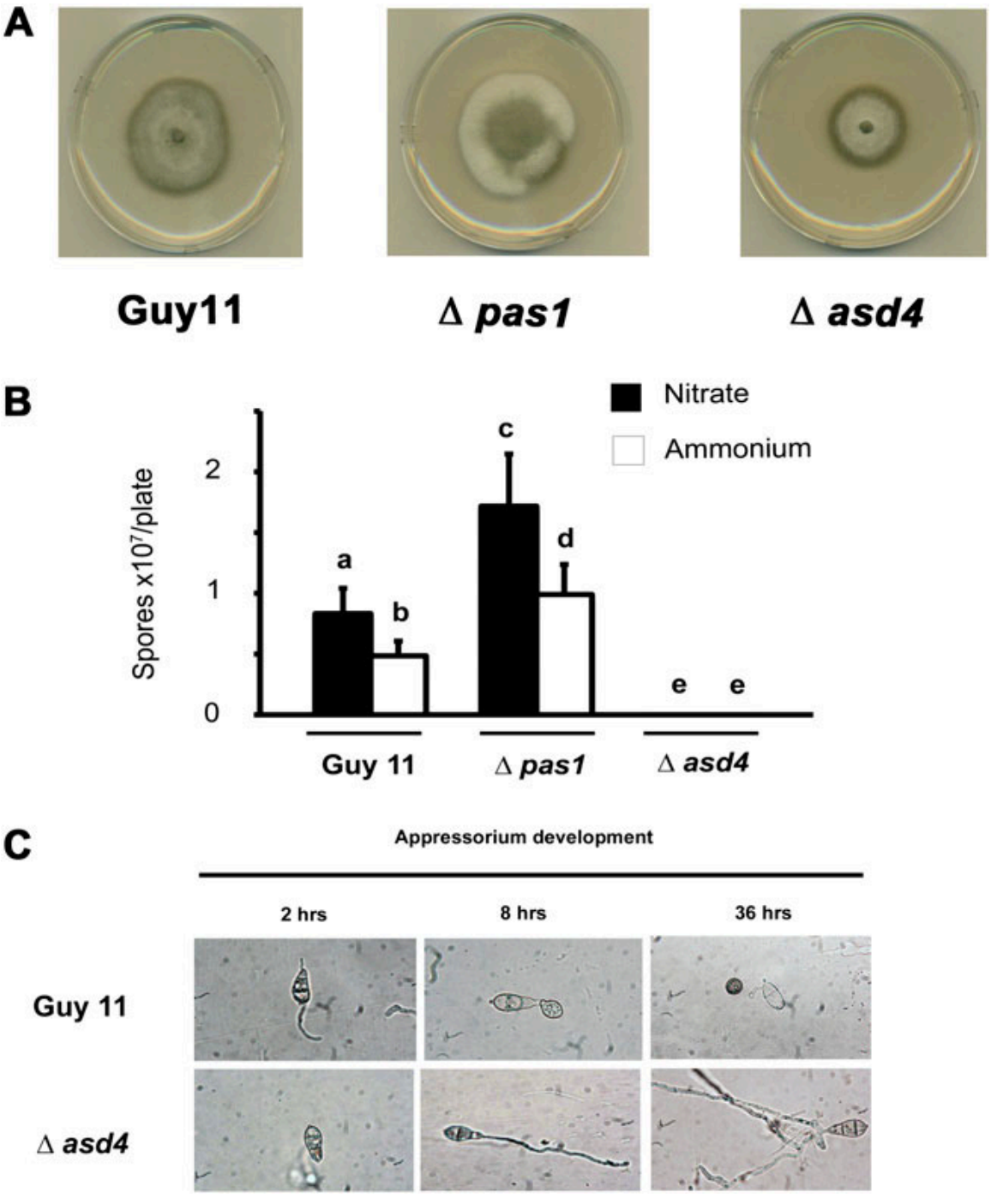
A
Guy11
Δ pas1
Δ asd4
B
Nitrate
Ammonium
Spores x10⁷/plate
0
1
2
a
b
c
d
e
e
Guy 11
Δ pas1
Δ asd4
C
Appressorium development
2 hrs
8 hrs
36 hrs
Guy 11
Δ asd4

Fig. S6

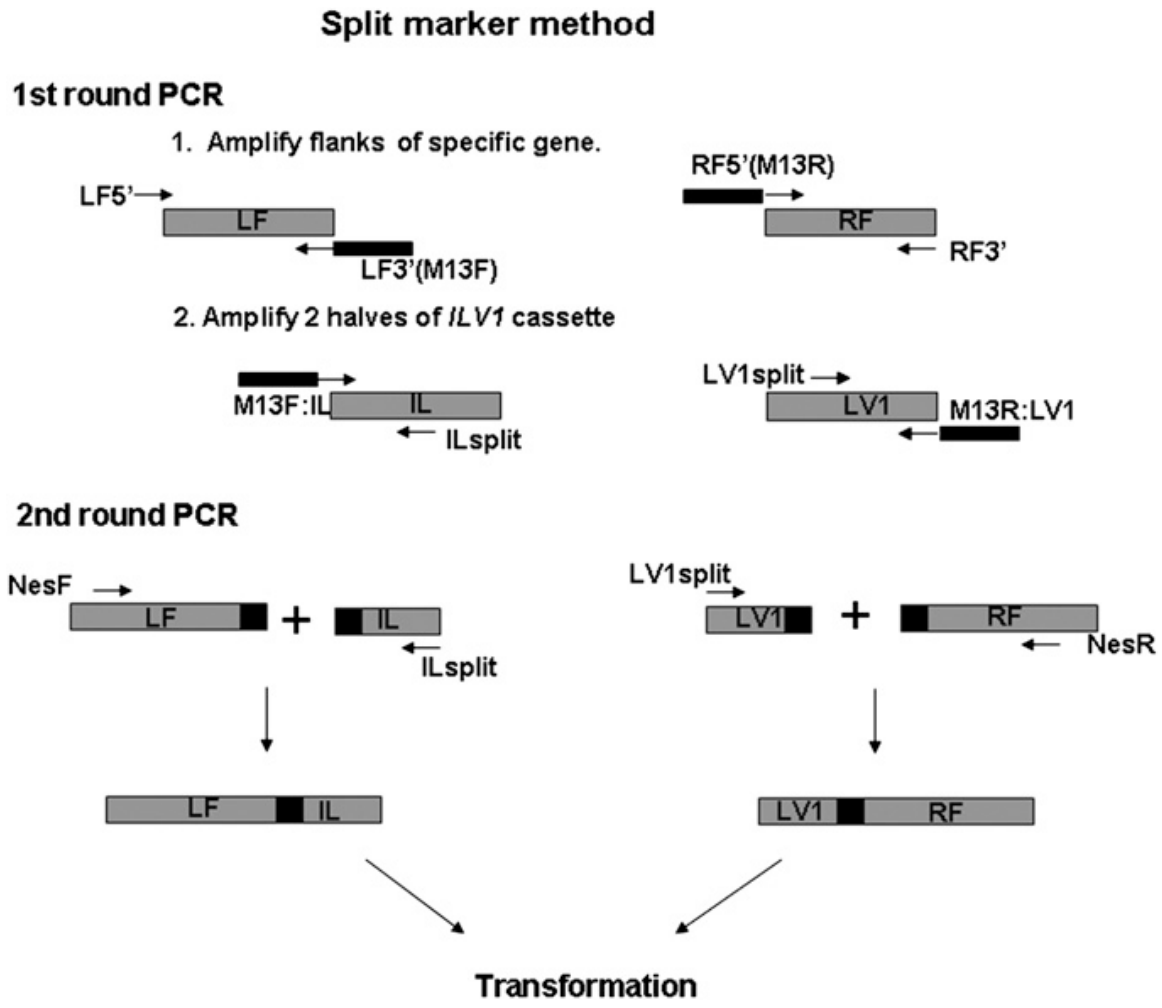
Split marker method
1st round PCR
1. Amplify flanks of specific gene.
LF5'
LF
LF3'(M13F)
RF5'(M13R)
RF
RF3'
2. Amplify 2 halves of ILV1 cassette
M13F:IL
IL
ILsplit
LV1split
LV1
M13R:LV1
2nd round PCR
NesF
LF
IL
ILsplit
LV1split
LV1
RF
NesR
LF
IL
LV1
RF
Transformation

Table S1.

Locus	*M. oryzae* Gene Name	Reference	Molecular function	Function reference
MGG_03860	*TPS1*	1, 2	Trehalose-6-phosphate synthase	3
MGG_02755	*NUT1*	4	GATA factor nitrogen regulatory protein	5
MGG_06062	*NIA1*	2	Nitrate reductase	6
MGG_01518	*NIR1*	*This study*	Nitrogen regulatory protein	7
MGG_00537	*MEP1*	*This study*	[a] Ammonium transporter	8
MGG_05526	*MEP2*	*This study*	[a] Ammonium transporter	8
MGG_00156	*NMR1*	2	NmrA-Like family	9
MGG_02860	*NMR2*	*This study*	NmrA-Like family	9
MGG_09705	*NMR3*	*This study*	NmrA-Like family	9
MGG_15113	*ALD1*	*This study*	[a] NADPH-dependent aldo/ keto reductases	10
MGG_07661	*KEF1*	*This study*	Kef-type K+ transport system[a]	11
MGG_10910	*SDY1*	*This study*	[a] NADPH-dependent short chain dehydrogenase	12
MGG_05940	*OXD1*	*This study*	[a] NADPH-dependent short chain dehydrogenase	12
MGG_07219	*ALB1*	13	Melanin biosynthesis	13
MGG_03817	*MPT1*	*This study*	[a] Metalloprotease	14
MGG_10315	*MPG1*	15	Hydrophobin	15

MGG_08297	*OYE1*	*This study*	[a] NADPH-dehydrogenase	16
MGG_06050	*ASD4*	*This study*	[a] GATA-type zinc finger protein	5
MGG_04521	*PAS1*	*This study*	[a] GATA-type zinc finger protein	5
MGG_01840	*SRE1*	*This study*	[a] GATA-type zinc finger protein	5
MGG_09926	*G6PDH*	*This study*	Glucose 6 phosphate dehydrogenase	17
MGG_00604	*TUB2*	*This study*	Tubulin β chain	18

Table S1. Description of *M. oryzae* genes analysed in this study. [a] Putative function based on sequence homology.

1. Foster AJ, Jenkinson JM, Talbot NJ (2007) Trehalose synthesis and metabolism are required at different stages of plant infection by *Magnaporthe grisea*. *EMBO J* 22: 225-235.

2. Wilson RA, Jenkinson JM, Gibson RP, Littlechild JA, Wang, ZY, Talbot NJ (2007) Tps1 regulates the pentose phosphate pathway, nitrogen metabolism and fungal virulence. *EMBO J* 26: 3673-3685.

3. Campbell JA, Davies GJ, Bulone V, Henrissat BA (1997) Classification of nucleotide-diphospho-sugar glycosyltransferases based on amino acid sequence similarities. *Biochem J* 326: 929-939.

4. Froeliger EH, Carpenter BE (1996) NUT1, a major nitrogen regulatory gene in *Magnaporthe grisea*, is dispensable for pathogenicity. *Mol Gen Genet* 251: 647-656.

5. Omichinski JG, Clore GM, Schaad O, Felsenfeld G, Trainor C, Appella E, Stahl SJ, Gronenborn AM (1993) NMR structure of a specific DNA complex of Zn-containing DNA binding domain of GATA-1. *Science* 261: 438-446.

6. Hyde GE, Crawford NM, Campbell W (1991) The sequence of squash NADH:nitrate reductase and its relationship to the sequences of other flavoprotein oxidoreductases. A family of flavoprotein pyridine nucleotide cytochrome reductases. *J Biol Chem* 266: 23542-23547

7. Berger H, Basheer A, Böck S, Reyes-Dominguez Y, Dalik T, Altmann F, Strauss J. Dissecting individual steps of nitrogen transcription factor cooperation in the *Aspergillus nidulans* nitrate cluster. *Mol Microbiol* 69: 1385-1398.

8. Marini AM, Soussi-Boudekou S, Vissers S, Andre B (1997) A family of ammonium transporters in *Saccharomyces cerevisiae*. *Mol Cell Biol* 17: 4282-4293.

9. Stammers DK, Ren J, Leslie K, Nichols CE, Lamb HK, Cocklin S, Dodds A, Hawkins AR (2001) The structure of the negative transcriptional regulator NmrA reveals a structural superfamily which includes the short-chain dehydrogenase/reductases. *EMBO J* 20: 6619-26.

10. Bohren KM, Bullock B, Wermuth B, Gabbay KH The aldo-keto reductase superfamily. cDNAs and deduced amino acid sequences of human aldehyde and aldose reductases. *J Biol Chem* 264: 9547-9551.

11. Ness LS, Booth IR (1999) Different foci for the regulation of the activity of the KefB and KefC glutathione-gated K+ efflux systems. *J Biol Chem* 274: 9524-9530.

12. Jörnvall H, Persson B, Krook M, Atrian S, Gonzàlez-Duarte R, Jeffery J, Ghosh D (1995) Short-chain dehydrogenases/reductases (SDR). *Biochemistry* 34: 6003-6013.

13. Chumley FG, Valent B (1990) Genetic analysis of melanin deficient non-pathogenic mutants of *Magnaporthe grisea. Mol Plant Microbe Interact* 3**:**135–143.

14. Baumann U, Wu S, Flaherty KM, McKay DB (1993) Three-dimensional structure of the alkaline protease of *Pseudomonas aeruginosa*: a two-domain protein with a calcium binding parallel beta roll motif. *EMBO J* 12: 3357-3364.

15. Talbot NJ, Ebbole DJ, Hamer JE (1993) Identification and characterization of MPG1, a gene involved in pathogenicity from the rice blast fungus *Magnaporthe grisea*. *Plant Cell* 5: 1575-1590.

16. Williams RE, Bruce NC (2002) 'New uses for an Old Enzyme' – the Old Yellow Enzyme family of flavoenzymes. *Microbiology* 148: 1607-1614.

17. Cosgrove MS, Naylor C, Paludan S, Adams MJ, Levy HR (1998) On the mechanism of the reaction catalyzed by glucose 6-phosphate dehydrogenase. *Biochemistry* 37: 2759-2767.

18. Nogales E, Wolf SG, Downing KH (1998) Structure of the alphabeta tubulin dimer by electron crystallography. *Nature* 391:199-203.

Chapter TWO

Upregulation of Tor-dependent pathways are associated with loss of virulence in the rice blast fungus

Reference:

Cristian F. Quispe, Anya A. Seng, Nandakumar Madayiputhiya, Richard A. Wilson

Upregulation of the Tor-dependent pathways are associated with loss of virulence in the rice blast fungus. Molecular Microbiology. *In preparation*.

ABSTRACT

Magnaporthe oryzae is arguably a devastating rice pathogen. The initiation of rice blast disease requires a regulatory mechanism involving an NADPH sensor protein trehalose-6-phosphate synthase 1 (Tps1), a set of NADP-dependent transcriptional corepressors and the nonconsuming interconversion of NADPH and NADP acting as signal transducer.

In *M. oryzae*, some GATA transcription factors control pathogenicity-associated gene expression through the Tps1 NADP-dependent transcriptional corepressors (Nmr proteins) and are essential for disease progression. Physical interactions occur between the Nmr proteins and at least three GATA transcription factors Nut1, Asd4 and Pas1. Gene functional analysis demonstrated that Asd4 is essential for pathogenicity.

In this study we elucidated the role of Asd4 as important regulator of the Tor signaling pathway that integrates important processes such as regulation of transcription, translation, ribosome biogenesis, trafficking and regulation of Golgi, secondary metabolism, autophagy and nitrogen metabolism.

We concluded that inactivation of the Tor kinase is essential to the initiation of infection-associated autophagy, and this mechanism might also interact with other signaling pathways such as G6P sensing by Tps1, cAMP-dependent protein kinase A and/or the membrane-associated heterotrimeric G proteins during appressorium morphogenesis and plant infection in the rice blast fungus.

Key words: Tor, GATA transcription factor, Asd4, Tps1

INTRODUCTION

Fungal plant pathogens of the ascomycete genus *Magnaporthe* are arguably devastating pathogens of several plants. They cause destructive and economically significant diseases on important species such as the monocotyledons rice, wheat and grasses. The most notorious *Magnaporthe* species is *M. oryzae*, the rice blast pathogen and a recurrent threat to world agriculture [56, 53, 38, 17].

Infection begins when the specialized infection structure, the appressorium, develops on a hydrophobic surface of the leaf and generates enormous internal turgor pressure through the accumulation of glycerol. This turgor acts on a penetration peg emerging at the base of the cell, causing it to breach the leaf surface allowing infection. Understanding how this process of infection is regulated is key to developing durable control strategies against rice blast [56, 47, 28, 27, 20, 7].

The initiation of rice blast disease requires a regulatory mechanism involving an NADPH sensor protein trehalose-6-phosphate synthase 1 (Tps1), a set of NADP-dependent transcriptional corepressors and the nonconsuming interconversion of NADPH and NADP acting as signal transducer [54, 52, 20, 18].

Nmr proteins are NADP-dependent transcriptional inhibitors and in *M. oryzae* they are controlled by Tps1. The Tps1-dependent Nmr inhibitor proteins regulate the expression of GATA-family transcription factors [54]. In eukaryotic organisms, GATA transcription

factors are well-studied gene activators involved in important cellular and metabolic processes [50, 48, 45, 34, 25, 12, 5, 4].

In *M. oryzae*, some GATA transcription factors control pathogenicity-associated gene expression through Tps1 and are essential for disease progression. Physical interactions occur between the Nmr proteins and at least three GATA transcription factors Nut1, Asd4 and Pas1. Gene functional analysis of *ASD4* showed it is essential for pathogenicity and also that Δ*asd4* mutant strains were significantly reduced in sporulation and radial growth [54].

In this study, we set out to determine the role of Asd4 in plant infection by *M. oryzae*. We decided to explore, in particular, the role of Asd4 as a nutrient sensor and its requirement for fungal pathogenicity. Here, we present evidence that the inability of *M. oryzae* Asd4 to cause disease is due to misregulation of ribosomal proteins expression, elevated retrograde golgi trafficking, loss of autophagy, and reduced GOGAT activity; all processes controlled by the Tor starvation pathway. We conclude that the role of Asd4 in fungal pathogenicity results from the upregulation of some Tor kinase-dependent pathways.

Furthermore, Asd4 controls the expression of nitrogen-regulated genes, and these findings lead us to conclude that in *M. oryzae*, nitrogen catabolite repression (NCR) is more similar to yeast than to other filamentous fungi. Taken together, our results demonstrate that the GATA factor Asd4 is an important regulator of Tor and essential for disease progression in the rice blast fungus.

RESULTS

Loss of appressorium formation in Δ*asd4* strains is not remediated by the addition of cAMP

Appressorium morphogenesis is a commitment step triggered by a hard, hydrophobic surface and the absence of exogenous nutrients. Δ *asd4* mutant spores are unable to make appressoria and instead make undifferentiated germ tubes that fail to hook or respond to the contact surface. The signal cyclic AMP (cAMP) pathway is important for appressorium morphogenesis. Addition of exogenously applied cAMP induces appressorium formation in mutants that lack the enzyme adenylate cyclase, allowing them to complete appressorium development. Similarly, addition of exogenous cAMP can restore appressorium development to wild type levels in the Δ*magB* mutant strain. MagB is a heterotrimeric G protein and a component in the early stages of appressorium formation [56, 35, 33, 17, 1].

To investigate how Asd4 might regulate fungal virulence, we tested if Δ*asd4* mutant spores would have a similar phenotype to mutants of the enzyme adenylate cyclase or magB by adding exogenous cAMP to Asd4 spores on plastic and glass coverslips (Fig. 1). We determined that the appressorium developmental defects associated with Δ*asd4* mutants cannot be overcome by addition of cAMP, which demonstrates that Asd4 operates either downstream of the cAMP and membrane-associated heterotrimeric G proteins - or in a different signaling network [6].

Asd4 and Nut1 discriminates between preferred and less preferred nitrogen sources in *Magnaporthe oryzae*

Microorganisms undergo major shifts in their transcriptional profile in response to changes in the surrounding nutrients. One essential nutrient for growth is nitrogen. The major transcription factors regulating nitrogen gene expression in most fungal species studied belong to the GATA-family transcription factors [51, 32, 31, 26, 24, 23, 14, 13, 11, 2] so we wonder if Asd4 might have a role in regulating nitrogen assimilation in *M. oryzae*.

Nitrogen utilization has global and complex regulation. The mechanism ensures that when excess of preferred or good nitrogen sources are available, such as glutamine or ammonium, cells inactivate GATA-family transcription factors that activate genes for assimilating less preferred or poor nitrogen sources. Another set of GATA transcription factors act as repressors of the same genes. On the other hand, in the absence of preferred or good nitrogen sources, and when cells are grown in the presence of less preferred or poor nitrogen sources, the positive acting GATA transcription factors are activated, and the repressors inactivated, leading to the expression of genes required for alternative nitrogen source metabolism [55, 46, 36, 15]. In *Saccharomyces cerevisiae* there are two distinct systems: one that discriminates the quality of available nitrogen sources, and a second that responds to the complete absence of nitrogen. The discriminatory pathway is activated after rapamycin treatment. In this pathway, Gln3 is a positively-acting transcription factor and the initial regulator that responds to nitrogen availability in the environment, therefore the major point of control for NCR. Gln3 is inactive in the cytoplasm in the presence of a good nitrogen source, but migration to the nucleus occurs

during growth on a poor nitrogen source. Gln3 turn on expression of NCR-regulated genes such as Gat1, Dal80 and Gzf3, whose gene products interact independently or in concert to repress or activate genes to influence expression of nitrogen catabolic/metabolic genes [29, 14, 13, 11, 9].

Dal80 and Gzf3 have a negative role in controlling expression of genes involved in nitrogen catabolism. These proteins prevent expression of genes for utilization of secondary nitrogen sources as long as the preferred nitrogen sources, glutamine or ammonium, are available [50, 46, 32, 25]. Because Gln3, Gat1, Dal80 and Gzf3 are constitutively expressed, it is thought that regulation happens in cooperative and competitive way at the promoter binding sites [13, 11, 9].

In filamentous fungi, regulation of nitrogen catabolic genes is also mediated by GATA transcription factors. The *A. nidulans* AreA, *P. chrysogenum* NRE and *N. crassa* Nit2 proteins are positively acting GATA factors involved in nitrogen regulation. In *M. oryzae* the homologue of AreA, Nut1, was shown to be essential to assimilate poor nitrogen sources and functionally complemented of the *A. nidulands* AreA strains, but was not required for pathogenicity [30, 24, 21, 19, 10, 8, 3]. Interestingly, Tps1, an important regulator of infection-related gene expression, regulates Nut1 by inactivating the inhibitor proteins Nmr1, Nmr2 and Nmr3 [54]. In contrast, the *A. nidulands* AreB, *P. chrysogenum* NreB and *N. crassa* Asd4 have a negative role in controlling expression of genes involved in nitrogen metabolism and sexual development. The *areB gene* was identified through a selection involving suppression of an AreA loss-of-function phenotype. NreB could prevent NRE activity in *P. chrysogenum* because both recognize similar DNA-

binding sites; therefore its function was also related as a repressor of NRE. *N. crassa* Asd4 protein was not consistent with a role in nitrogen control however it was associated with the loss of ascospore production. Despite the discrepancies, phylogenetic analysis demonstrates that AreB, NreB and Asd4 are orthologous in the ascomycetes [24, 21, 19, 10].

In fungi, nitrogen catabolite repression (NCR) control is related with essential biological processes such as initiation of morphological changes, expression of virulence factors, or initiation of sexual and asexual sporulation. For instance, in *C. albicans* CaGcn4, played important role in coordinating morphogenetic and metabolic responses to amino acid starvation. Similarly, pathogenicity of *Aspergillus fumigatus* dependents on its ability to respond to limited nitrogen sources [45, 34, 26, 21].

Like most microorganisms, *M. oryzae* prefers some nitrogen sources to others. For instance glutamine, glutamate, asparagine and ammonium are good nitrogen sources that promote sustainable growth on axenic media over others sources such as nitrate, proline, histidine, or arginine (data not shown). Our data demonstrate that Δ*asd4* colony growth was slightly affected under poor nitrogen sources such as nitrate, proline, histidine, and arginine. However on good nitrogen sources, such glutamine, glutamate, asparagine and ammonium, a significant reduction in colony size was observed (Fig. 2A & 2B). The ability of Δ*asd4* to sense the quality of available nitrogen sources was independent of the carbon source. Therefore Asd4 only discriminates the quality of the nitrogen source rather than the quality of the nitrogen and the carbon source (Fig. 3) [50, 46, 32, 25].

In addition, we contrast the ability of Asd4 and Nut1 to assimilate different nitrogen

sources. Nut1 was reported as the major nitrogen regulatory protein in *M. oryzae*. Our data reports that on the nitrogen sources in which Δ*asd4* mutant strains show significant reduction in colony growth, Δ*nut1* demonstrate normal growth. Intriguingly, Nut1 is essential to assimilate poor nitrogen sources such as: nitrate, lysine, ornithine, glucosamine, proline, histidine, homocysteine, alanine and argnine; nitrogen sources in which Δ*asd4* mutant strains growth was only slightly affected.

Therefore, we suggest that NCR in *M. oryzae* is quite different to the model filamentous fungi *A. nidulans*, because in this fungus AreA controls the expresson of genes required for the metabolism of all less-preferred nitrogen sources, which is not the case for Nut1 in *M. oryzae.* Instead, NCR in *M. oryzae* ressembles the *S. cerevisiae* model, with nitrogen sources other than glutamine and ammonium being assimilated by either Nut1 or Asd4 [50, 46, 32, 25, 11, 9]. Because Asd4 controls the assimilation of good nitrogen we reasoned that Asd4 might also control the glutamate synthase or GS-GOGAT cycle.

Asd4 negatively regulate the Tor-dependent pathway

In *S. cerevisiae*, the availability of nitrogen and/or amino acids results in expression of their respective transporters for uptake mediated by the Tor (target of rapamycin) pathway, therefore nitrogen is a particularly important nutrient in Tor signaling [44-39,37, 16, 9].

Rapamycin highly affects nitrogen-regulated genes involved in the assimilation of alternative nitrogen sources and promotes nuclear accumulation of Gln3. In contrast, intracellular glutamine inhibits activation of Gln3 [43,42,9]. Thus, having established the role of Asd4 in good nitrogen sources assimilation we ask if Asd4 have a role in the Tor

pathway? Tor is the major nutrient-sensing pathway and in *S. cerevisiae* controls essential cellular processes [9]. While rapamycin inhibits wild type *M. oryzae* growth on minimal media, presumably through disrupting the Tor pathway, the Δ*asd4* mutant strain did not demostrate reduced growth in the presence of rapamycin compared to the absence. (Fig. 4). This suggests that inactivation of Tor by rapamycin requires Asd4 and therefore, Asd4 negatively regulates Tor-dependent pathways downstream of this signaling pathway. Intriguingly, following our model for roles of Asd4 and Nut1 in NCR, Nut1 mutant strains were more sensitive phenotype than the wild type to rapamycin treatment.

LC-MS/MS-based proteome profiling of Δ*asd4* strains confirms a role for Asd4 in the regulation of Tor-associated pathways

We next sought to understand the processes altered in Δ*asd4* strains by comparing their proteome to wild type strains. From about 872 identified proteins, we selected a total of 62 that showed at least 2-fold difference in expression between the wild type and the Δ*asd4* mutant strain. It is well established that the Tor signalling pathway controls changes to many cellular processes, such as translation, ribosomal biogenesis, mitochondrial activity, lipid biosynthesis, glycolysis and autophagy [44-39,37, 16, 9].

To highlight the important global protein expression profiles, we divided the set of proteins into four categories: genetic information processing, cellular processes, metabolism, and environmental cues (Fig. 5). MS analysis results are summarized in table S1. Firstly, strong evidences of misregulation of proteins involved in mRNA

processing, chromatin remodeling and posttranslational regulation were detected in the **Δ***asd4* mutant strain. Cellular process such as ribosome biogenesis, Golgi trafficking, mitochondrial structure were absent or upregulated in the mutant strain. Finally, proteins involved in nitrogen regulation, metabolism of some aminoacids, secondary metabolism, and carbon catabolite derepression also were disturbed.

Asd4 controls autophagy and suggests Δ*asd4* strains are constitutively upregulated for some Tor-dependent pathways

Finally, to demonstrate a role for Asd4 in autophagy, we compare fungal growth of wild type, Δ*asd4* and Δ*tps1* strains on minimal media supplemented with charcoal –ie reduced nutrient media. Δ*tps1* strains appear accelerated for growth on these poor-media tests, indicating autophagy is perhaps enhanced in the strains compared to wild type, whereas Δ*asd4* strains do not undergo autophagy and is consistent with our proteomics data (Fig. 6A). Therefore, Asd4 is required for autophagy, and autophagy is negatively regulated by Tor [43, 42, 41]. Therefore, we conclude that in Δ*asd4* strains, Tor inactivation of autophagy is constitutive regardless of nutritional status, resulting in the inability to form appressoria on the surface of the plant, and an inability to adapt to the nutritional status of the plant tissue within the plant (Fig. 6B).

DISCUSSION

In this study we set out to understand the role of the GATA transcription factor Asd4 as an important regulator in the establishment of rice blast disease. When considered together, our results are consistent with a role for Asd4 as part of the Tor signaling pathway in *M. oryzae,* which is essential for virulence and integrates important processes such as regulation of transcription, translation, ribosome biogenesis, trafficking and regulation of Golgi, secondary metabolism, autophagy and nitrogen metabolism [44-39,37, 16, 9].

Elucidation of the Asd4 regulatory mechanism confirms the importance of the nutrient-sensing ability of plant pathogens to adapt their life style to the changing-environment. We demonstrate that NCR gene expression in *M. oryzae* is regulated by a complex regulatory system involving, so far, two GATA family transcription factors, Asd4 and Nut1. Nut1 is essential for expression of NCR genes that mediates the assimilation of poor nitrogen sources [20]. In contrast, Asd4 is necessary for the assimilation of preferred nitrogen sources through control of the GOGAT pathway. Such regulation of the GOGAT pathway is likely to also regulate the Tor pathway. In *S. cerevisiae* the finding that glutamine controls Tor signaling highlight the importance of glutamine, therefore GOGAT, in nitrogen metabolism. In *M. oryzae*, previous studies suggested that inhibition of NCR is necessary to induce rice blast disease, however we suggest that it is the fine-tuning genetic control of GATA factors involved in NCR that are necessary to accomplish successful infection of the rice blast fungus.

We speculate that this adaptability to fluctuating nutritional environments is necessary in

plant pathogens such as *M. oryzae* which must quickly adapt from a nutrient-free environment to a rich-intracellular living plant tissue, where a rapid genetic re-programming needs to happen, presumably at the NCR level, in order to evade or suppress the host defense response to establish disease [56, 53, 38, 17].

The results presented here suggest that *M. oryzae* NCR control acts similarly to the NCR model in *S. cerevisiae*, where the expression of GATA factors is necessary to active and/or repress nitrogen metabolism [29, 14, 13, 11, 9].

The nitrogen regulation also seems to be linked to the Tor signaling pathway and may be responsible for appressorium morphogenesis because Δ*asd4* strains do not form appressoria. Significantly, inactivation of the Tor pathway and its control on autophagy by Asd4 suggest it has important roles in disease development in *M. oryzae* [28]. Therefore it is highly informative that inactivation of Tor kinase is essential to the initiation of infection-associated autophagy, and in the future we will explore how this mechanism might also interact with other signaling pathways such as G6P sensing by Tps1, cAMP-dependent protein kinase A and/or the membrane-associated heterotrimeric G proteins during appressorium morphogenesis [6], all processes necessary for appressorium morphogenesis and plant infection in the rice blast fungus.

MATERIALS AND METHODS

Strains, physiological tests and plant infections

All strains were derived from the wild type Guy11 (Table S2). Strains were maintained on complete medium (CM) containing 1 % (W/V) glucose, 0.2 % (W/V) peptone, 0.1 % (W/V) yeast extract and 0.1 % (W/V) casamino acids, or on minimal medium (MM) containing 50 mM of the respective carbon sources and 10 mM of the stated nitrogen source, as described in (Wilson et al., 2007). All carbon and nitrogen sources were added to MM in the amounts indicated after autoclave the media. Plate images were scanned with a HP Scanjet G3110 Scanner, 4800 x 9600 dpi and 48-bit color.

For nutritional plate test, 10 mm^2 blocks of mycelium were transferred to the centre of each 90×15mm petri dish, and the strains grown for 16-18 days at 26 ^oC with 12 hr light/ dark cycles. Colony diameters were measured using ImageJ free software from NIH.

Rapamycin was added to ammonium acetate minimal media at a concentration of 55 ng/mL and the strains grown for 7-9 days in 50 x 12mm petri dishes. Activated charcoal (3% w/v) was added to ammonium acetate minimal media and the strains grown for 5 days in petri dishes.

Appressoria development was analyzed by inoculating a 240 µl droplet of water containing 2 X 10^4 spores onto plastic and glass coverslips (Fisher) for development under hydrophobic and hydrophilic conditions. Monobutyryl cyclic AMP (mb-cAMP) was added to 10 mM as described in (Lee et al., 1993).

Images were taken using a Nikon Eclipse 50i microscope and a Nikon DS-Fi1 Digital Sight camera and were analyzed using ImageJ free software from NIH.

Rice plant infections were made using a susceptible Indica rice (*Oryza sativa*) cultivar, CO-39 using the rub-inoculation method (Carborundum-dusted) to disrupt the cell walls. Fungal spores were isolated from 12 –14 day-old plate cultures and spray-inoculated onto rice plants of cultivar CO-39 in 0.2 % gelatin at a concentration of 5 x 10^5 spores / ml, and disease symptoms were allowed to develop under conditions of high relative humidity for 5-7 days, as described in (Wilson, et al., 2010).

Protein extraction and LC/MS/MS analysis

Proteomic extraction was performed as follows. Strains were grown in CM for 48 hrs, then transferred to MM with nitrate for 16 hrs, as described in (Wilson et al., 2010). Five hundred mg (500 mg) of fungal biomass (wet weight) was transferred into a 1mL lysis buffer (8M urea in 100 mM ammonium bicarbonate containing bead 1.5 mM protease inhibitor PMSF, Sigma, USA). The biomass was then subjected to bead beating using glass bead beater for 3 min / 4^{o}C. Supernatant was collected after centrifugation for 10000g / 20 min and treated by cold acetone precipitation. 9 ml of acetone was added to 1 ml of sample, and the proteins allowed to precipitate overnight at -20 ^{o}C. The resulting precipitate was collected by centrifugation at 7000 x g for 30 min and airdried to remove residual acetone. The dried pellets were resolubilised in 250 µl of 100 mM ammonium bicarbonate and the protein concentration was estimated using the BCA protein assay kit (Thermo Fisher Scientific, USA). The dried pellets were resuspended in 250uL of 100

mM ammonium bicarbonate and the protein concentration was estimated using BCA assay.

For the LC/MS/MS analysis, in solution trypsin digestion was performed on the extracted fungal protein using the protocol described in (Nandakumar et al 2011). After 16 hrs of tryptic digestion the reaction was terminated by adding 0.1% formic acid. The peptide solution was later dried using speed vacuum drier (Thermo fisher, USA) and reconstituted with 20uL of 0.1% formic acid in water. The collected samples were subjected to LC/MS/MS analysis.

Fully automated, on-line one dimensional LC/MS/MS was carried out with a ultimate 3000 Dionex nano LC system (Dionex corporation, USA) integrated with LCQ Fleet Ion Trap mass spectrometer (Thermo scientific, USA) and equipped with a nano source. The method included an on-line sample preconcentration and desalting step using a monolithic C 18 – trap column (Pep Map, 300 um I.D, 5 um, 100A, 1mm monolithic C 18 column, Dionex Corporation USA). Loading and desalting of the sample on the trap column was conducted using a loading pump at a flow rate of 40 uL/ min with mobile phase A (water plus 0.1% formic acid). The desalted peptides were then eluted and separated on a C18 Pep Map column, (Dionex 75 um I.Dx15 cm, 3 um, 100A, Dionex Corporation, USA) by applying an acetonitrile gradient from 0 to 95% (mobile phase B, acetonitrile plus 0.1% formic acid). The total run time was 90 min including 25 min re-equilibration at a flow rate of 300 nL/min. The eluted peptides were directly introduced into the mass spectrometer using a nano source in on-line fashion. The LCQ fleet mass spectrometer was operated with the following parameters: nano spray voltage (2.0 kV),

heated capillary temperature of 200 °C, full scan m/z range 400-2000. The LCQ was operated in a data dependent mode with 35% collision energy for collision induced dissociation.

The acquired MS/MS spectrum was searched against *M. oryzae* protein sequence database (NCBI) using MASCOT (Matrix Sciences, UK) bioinformatics software to identify the protein and Scaffold software for further spectrum counting and protein quantitative analysis.

REFERENCES

1. Adachi K, Hamer JE (1998) Divergent cAMP signaling pathways regulate growth and pathogenesis in the rice blast fungus *Magnaporthe grisea*. Plant Cell 10:1361–73.

2. Arst HN, Cove DJ (1973) Nitrogen metabolite repression in *Aspergillus nidulans*. Mol Gen Genet 126: 111–141.

3. Arst HN, Hondmann DA, Visser J (1990) A translocation activating the cryptic nitrogen regulation gene areB inactivates a previously unidentified gene involved in glycerol utilisation in *Aspergillus nidulans*. Mol Gen Genet 223: 134–137.

4. Ballance DJ (1986) Sequences important for gene expression in filamentous fungi. Yeast 2: 229–236.

5. Ballario P, Vittorioso P, Magrelli A, Talora C, Cabibbo A, Macino G (1996) White collar-1, a central regulator of blue light responses in *Neurospora*, is a zinc finger protein. EMBO J 15: 1650–1657.

6. Chen JC, Powers T. (2006) Coordinate regulation of multiple and distinct biosynthetic pathways by TOR and PKA kinases in S. cerevisiae. Curr Genet. 49, 281-293.

7. Chumley FG, Valent B (1990) Genetic analysis of melanin deficient non-pathogenic mutants of *Magnaporthe grisea*. Mol. Plant Microbe Interact 3: 135–143.

8. Conlon H, Zadra I, Haas H, Arst HN, Jones MG. and Caddick MX (2001) The *Aspergillus nidulans* GATA transcription factor gene *areB* encodes at least three proteins and features three classes of mutation. Molecular Microbiology, 40: 361-375.

9. Crespo JL, Powers T, Fowler B, Hall MN (2002) The TOR-controlled transcription activators GLN3, RTG1, and RTG3 are regulated in response to intracellular levels of glutamine. Proc Natl Acad Sci USA. 99 (10): 6784-8789.

10. Chae KS, Kim JH, Choi Y, Han DM, Jahng KY (1995) Isolation and characterization of a genomic DNA fragment complementing an nsdD mutation of *Aspergillus nidulans*. Mol Cells 5: 146–150.

11. Coffman JA, Rai R, Cunningham TS, Svetlov V, Cooper TG (1996) Gat1p, a GATA family protein whose production is sensitive to nitrogen catabolite repression participates in transcriptional activation of nitrogen-catabolic genes in *Saccharomyces cerevisiae*. Mol Cell Biol 16: 847–858.

12. Coffman JA, Rai R, Loprete DM, Cunningham T, Svetlov V, Cooper TG (1997) Cross regulation of four GATA factors that control nitrogen catabolic gene expression in *Saccharomyces cerevisiae.* J Bacteriol 179: 3416–3429.

13. Crawford NM, Arst HN (1993) The molecular genetics of nitrate assimilation in fungi and plants. Annu Rev Genet 27: 115–146.

14. Cunningham TS, Cooper TG (1991) Expression of DAL80, whose product is homologous to the GATA factors and is a negative regulator of multiple nitrogen catabolic genes in *Saccharomyces cerevisiae*, is sensitive to nitrogen catabolite repression. Mol Cell Biol 11: 6205–6215.

15. Cunningham TS, Rai R, Cooper TG (2000) The level of DAL80 expression down-regulates GATA factor-mediated transcription in *Saccharomyces cerevisiae.* J Bacteriol 182: 6584–6591.

16. Dilova I, Aronova S, Chen JCY, Powers T (2004) Tor signaling and nutrient-based signals converge on Mks1p phosphorylation to regulate expression of Rtg1p/Rtg3p-dependent genes. J. Biol. Chem. 279, 46527-46535.

17. Dean R A et al. (2005) The genome sequence of the rice blast fungus *Magnaporthe grisea.* Nature 434: 980-986.

18. Eastmond PJ, van Dijken AJ, Spielman M, Kerr A, Tissier AF, Dickinson HG, Jones JD, Smeekens SC, Graham IA (2002) Trehalose-6-phosphate synthase 1, which catalyses the first step in trehalose synthesis, is essential for Arabidopsis embryo maturation. Plant J 29: 225–235.

19. Feng B, Haas H, Marzluf GA (2000) ASD4, a new GATA factor of *Neurospora crassa*, displays sequence-specific DNA binding and functions in ascus and ascospore development. Biochemistry 39: 11065-11073.

20. Foster AJ, Jenkinson JM, Talbot NJ (2003) Trehalose synthesis and metabolism are required at different stages of plant infection by *Magnaporthe grisea*. EMBO J 22: 225-235.

21. Froeliger E H, Carpenter BE (1996) NUT1, a major nitrogen regulatory gene in *Magnaporthe grisea,* is dispensable for pathogenicity. Mol Gen Genet 251: 647-656.

22. Fu YH, Marzluf GA (1990) nit-2, the major nitrogen regulatory gene of *Neurospora crassa*, encodes a protein with a putative zinc finger DNA-binding domain. Mol Cell Biol 10: 1055–1065.

23. Haas H, Bauer B, Redl B, Stoffler G, Marzluf GA (1995) Molecular cloning and analysis of nre, the major nitrogen regulatory gene of *Penicillium chrysogenum.* Curr Genet 27: 150–158.

24. Haas H, Angermayr K, Zadra I, Stoffler G (1997) Overexpression of nreB, a new GATA factor-encoding gene of *Penicillium chrysogenum,* leads to repression of the nitrate assimilatory gene cluster. J Biol Chem 272: 22576–22582.

25. Haas H, Zadra I, Stoffler G, Angermayr K (1999) The *Aspergillus nidulans* GATA factor SREA is involved in regulation of siderophore biosynthesis and control of iron uptake. J Biol Chem 274: 4613–4619.

26. Han S, Navarro J, Greve RA, Adams TH (1993) Translational repression of brlA expression prevents premature development in *Aspergillus*. EMBO J 12: 2449–2457.

27. Kankanala P, Czymmek K, Valent B (2007) Roles for Rice Membrane Dynamics and Plasmodesmata during Biotrophic Invasion by the Blast Fungus. Plant cell 19: 706 – 724.

28. Kershaw MJ, Talbot NJ (2009) Genome-wide functional analysis reveals that infection-associated fungal autophagy is necessary for rice blast disease. Proc Natl Acad Sci U S A 106: 15967-15972.

29. Komeili A, Wedaman KP, O'Shea EK, Powers T (2000) Mechanism of metabolic control. Target of rapamycin signaling links nitrogen quality to the activity of the Rtg1 and Rtg3 transcription factors. J Cell Biol. 151(4):863-78.

30. Kozak M. (1999) Initiation of translation in prokaryotes and eukaryotes. Gene 234: 187–208.

31. Kudla B, Caddick MX, Langdon T, Martinez-Rossi NM, Bennett CF, Sibley S, et al. (1990) The regulatory gene areA mediating nitrogen metabolite repression in

Aspergillus nidulans. Mutations affecting specificity of activation alter a loop residue of a putative zinc finger. EMBO J 9: 1355–1364.

32. Kuruvilla FG, Shamji AF, Schreiber SL (2001) Carbon- and nitrogen-quality signaling to translation are mediated by distinct GATA-type transcription factors. Proc Natl Acad Sci USA vol. 98:7283–7288.

33. Lee YH, Dean RA (1993) cAMP Regulates lnfection Structure Formation in the Plant Pathogenic Fungus *Magnaporthe grisea.* The Plant Cell 5: 693-700.

34. Linden H, Macino G (1997) White collar 2, a partner in blue-light signal transduction, controlling expression of light-regulated genes in *Neurospora crassa*. EMBO J 16: 98–109.

35. Lau G, Hamer JE (1996) Regulatory Genes Controlling MPG1 Expression and Pathogenicity in the Rice Blast Fungus *Magnaporthe grisea*. Plant Cell 8: 771-781.

36. Lamb HK, Leslie K, Dodds AL, Nutley M, Cooper A, Johnson C, Thompson P, Stammers DK, Hawkins, AR (2003) The Negative Transcriptional Regulator NmrA Discriminates between Oxidized and Reduced Dinucleotides. J Biol Chem 278: 32107–32114.

37. Martin DE, Powers T, Hall MN (2006) Regulation of ribosome biogenesis; Where is TOR? Cell Metabolism 4, 259-260.

38. Pennisi E (2010) Armed and Dangerous Science 327: 804-805.

39. Powers T, Walter P (1999) Regulation of ribosome biogenesis by the rapamycin-sensitive TOR-signaling pathway in *Saccharomyces cerevisiae.* Mol Biol Cell. 10(4):987-1000.

40. Powers T, Chen CY, Dilova D, Reinke A, Wedaman KP (2004) Tor-signaling and Tor-interacting proteins in yeast. Topics in Current Genetics 7, 201-223.

41. Powers T, Dilova I, Chen CY, Wedaman K (2004) Yeast TOR signaling: a mechanism for metabolic regulation. Curr Top Microbiol Immunol.

42. Powers T. (2004) Ribosome Biogenesis: Giant Steps for a Giant Problem. Cell, Vol 119, 901-902.

43. Powers T. (2008) Cell growth control:mTOR takes on fat. Mol. Cell 31, 775-776.

44. Powers T (2007) TOR Signaling and S6 Kinase 1: Yeast Catches Up. Cell Metabolism 6, 1-2.

45. Scazzocchio C (2000) The fungal GATA factors. Curr Opin Microbiol 3: 126–131.

46. Soussi-Boudekou S, Vissers S, Urrestarazu A, Jauniaux JC, Andre B. (1997) Gzf3p, a fourth GATA factor involved in nitrogen-regulated transcription in *Saccharomyces cerevisiae.* Mol Microbiol 23: 1157–1168.

47. Talbot NJ, Ebbole DJ, Hamer JE (1993) Identification and characterization of MPG1, a gene involved in pathogenicity from the rice blast fungus *Magnaporthe grisea.* Plant Cell 5: 1575-1590.

48. Teackle GR, Gilmartin PM (1998) Two forms of type IV zinc-finger motif and their kingdom-specific distribution between the flora, fauna and fungi. Trends Biochem Sci 23: 100–102.

49. Tollervey DW, Arst HN (1982) Domain-wide, locus-specific suppression of nitrogen metabolite repressed mutations in *Aspergillus nidulans.* Curr Genet 6: 79–85.

50. Wiame JM, Grenson M, Arst, HN (1985) Nitrogen catabolite repression in yeasts and filamentous fungi. Adv Microb Physiol 26: 1–88.

51. Wilson RA, Arst HN (1998) Mutational analysis of AREA, a transcriptional activator mediating nitrogen metabolite repression in *Aspergillus nidulans* and a member of the "streetwise" GATA family of transcription factors. Microbiol Mol Biol Rev 62: 586-596.

52. Wilson RA, Jenkinson, JM, Gibson, RP, Littlechild, JA, Wang, ZY, Talbot, NJ (2007) Tps1 regulates the pentose phosphate pathway, nitrogen metabolism and fungal virulence. EMBO J 26: 3673-3685.

53. Wilson RA, Talbot NJ (2009) Under pressure: investigating the biology of plant infection by the rice blast fungus *Magnaporthe oryzae*. Nature Rev Microbiol. 7: 185-195.

54. Wilson RA, Gibson RP, Quispe CF, Littlechild JA, Talbot NJ (2010) An NADPH-dependent genetic switch regulates plant infection by the rice blast fungus. Proc Natl Acad Sci USA. 107: 21902–21907.

55. Wong KH, Hynes MJ, Todd RB, Davis MA (2009) Deletion and overexpression of the *Aspergillus nidulans* GATA factor AreB reveals unexpected pleiotropy.

Microbiology 155: 3868–3880.

56. Talbot NJ (2003) On the trail of a cereal killer: Exploring the biology of *Magnaporthe grisea*. Annu Rev Microbiol 57:177-202.

FIGURE LEGENDS

Fig 1. Loss of appressorium formation in Δ*asd4* strains is not remediated by the addition of cAMP. A) Appressoria development was analyzed by inoculating a 240 µl droplet of water containing 2 X 10^4 spores onto plastic and glass coverslips for development under hydrophobic and hydrophilic conditions. B) Monobutyryl cyclic AMP (mb-cAMP) was added to 10 mM as described in (Lee et al., 1993).

Fig 2. Asd4 discriminates between preferred and less preferred nitrogen sources in *Magnaporthe oryzae.* A) Plate tests of nitrogen utilization by Guy11 and Δ *asd4* strains in the presence of glucose. Strains were grown for 16-18 days on minimal media containing 50 mM glucose supplemented with 10 mM of the indicated nitrogen source. B) Percentage of the diameters of the Δ *asd4* strains grown on the indicated media compared to the wild type strain.

Fig 3. Asd4 discriminates between preferred and less preferred nitrogen sources regardless of the carbon source. Plate tests of different nitrogen and carbon sources by Guy11 and Δ *asd4*. Strains were grown for 16-18 days on minimal media containing 50 mM of the indicated carbon source and 10 mM of the indicated nitrogen source.

Fig 4. Asd4 negatively regulate the Tor-dependent pathway. Plate tests of Guy11, Δ*nut1* and Δ *asd4* mutant strains on minimal medium containing 55 ng/mL of rapamycin. Strains were grown for 8 days.

Fig 5. LC-MS/MS-based proteome profiling of Δ*asd4* strains confirms a role for Asd4 in the regulation of Tor-associated pathways. Global protein expression profiles

that indicated the disturbed processes in the *Δ asd4* strains compared with the wild type Guy11.

Fig 6. Asd4 controls autophagy and suggest upregulation of the Tor-dependent pathway. A) Plate tests of Guy11, Δ *tps1* and Δ *asd4* mutant strains on minimal medium containing 50 mM of glucose, 10 mM of ammonium acetate and activated charcoal (3% w/v). Strains were grown for 5 days. B) Fungal spores were isolated from 12 –14 day-old plate cultures and spray-inoculated onto rice plants of cultivar CO-39 in 0.2 % gelatin at a concentration of 5 x 10^5 spores / mL using the rub-inoculation method (Carborundum-dusted) to disrupted the cell walls.

Fig. 1. Loss of appressorium formation in Δ*asd4* strains is not remediated by the addition of cAMP.

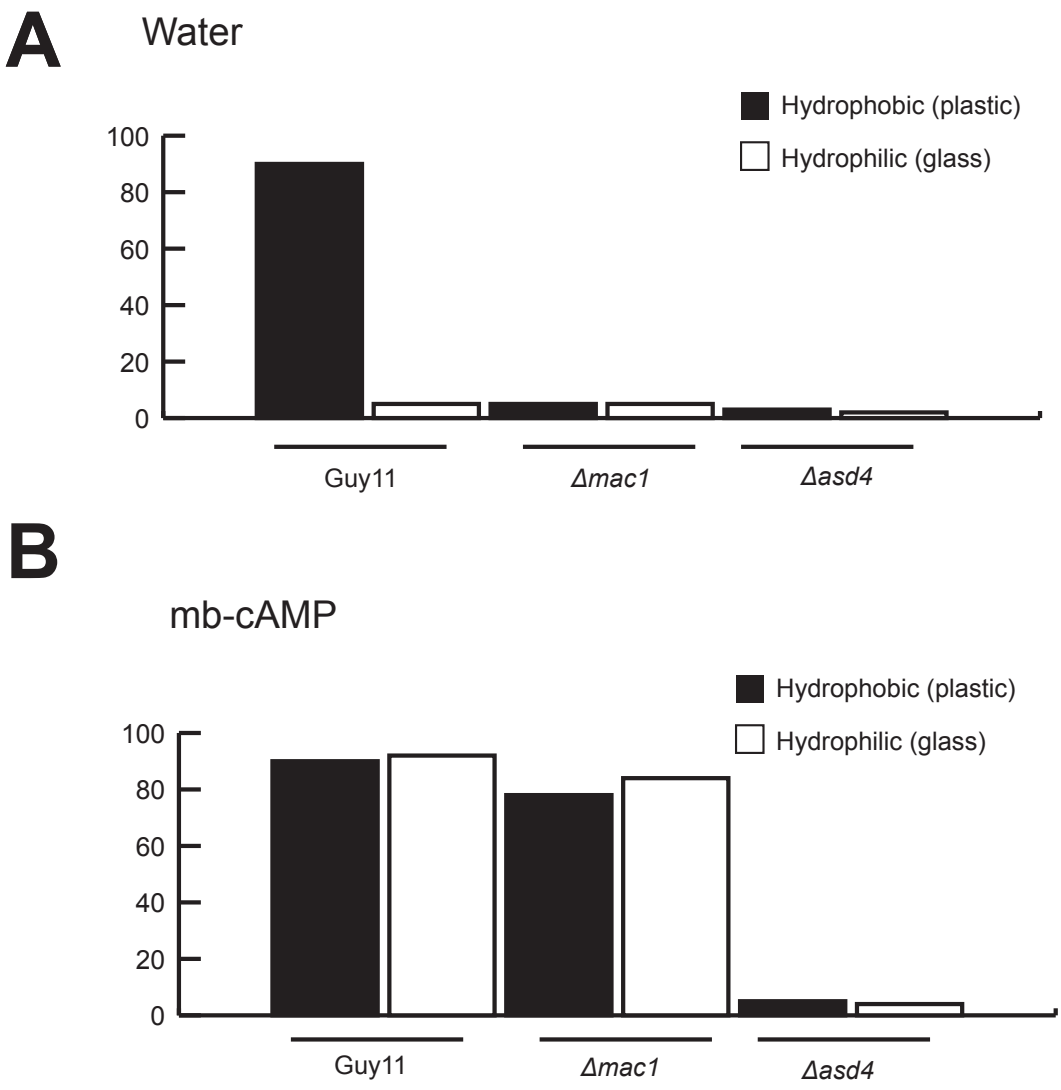

Fig. 2. Asd4 discriminates between preferred and less preferred nitrogen sources in *Magnaporthe oryzae.*

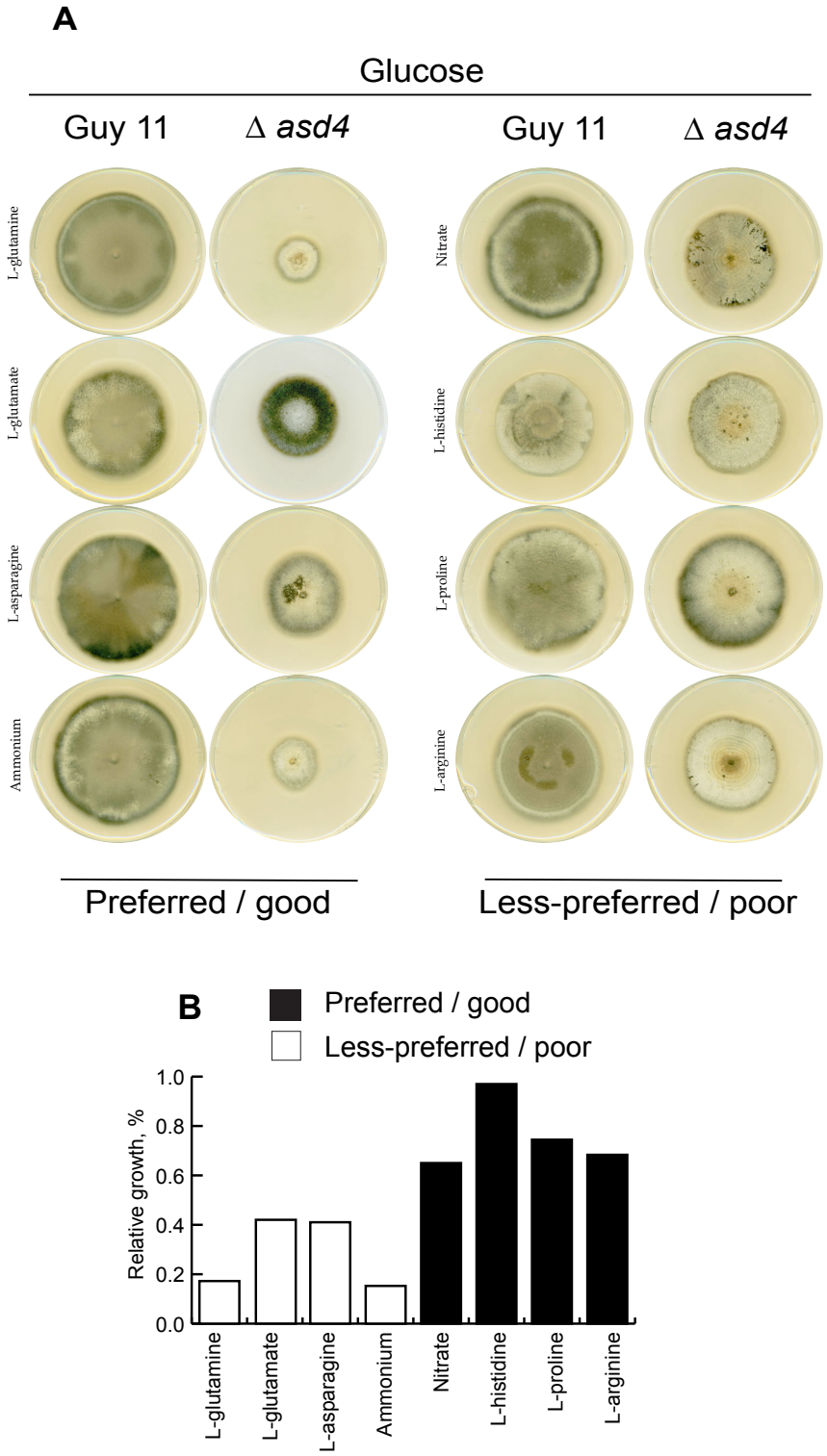

Fig. 3. Asd4 discriminates between preferred and less preferred nitrogen sources regardless of the carbon source.

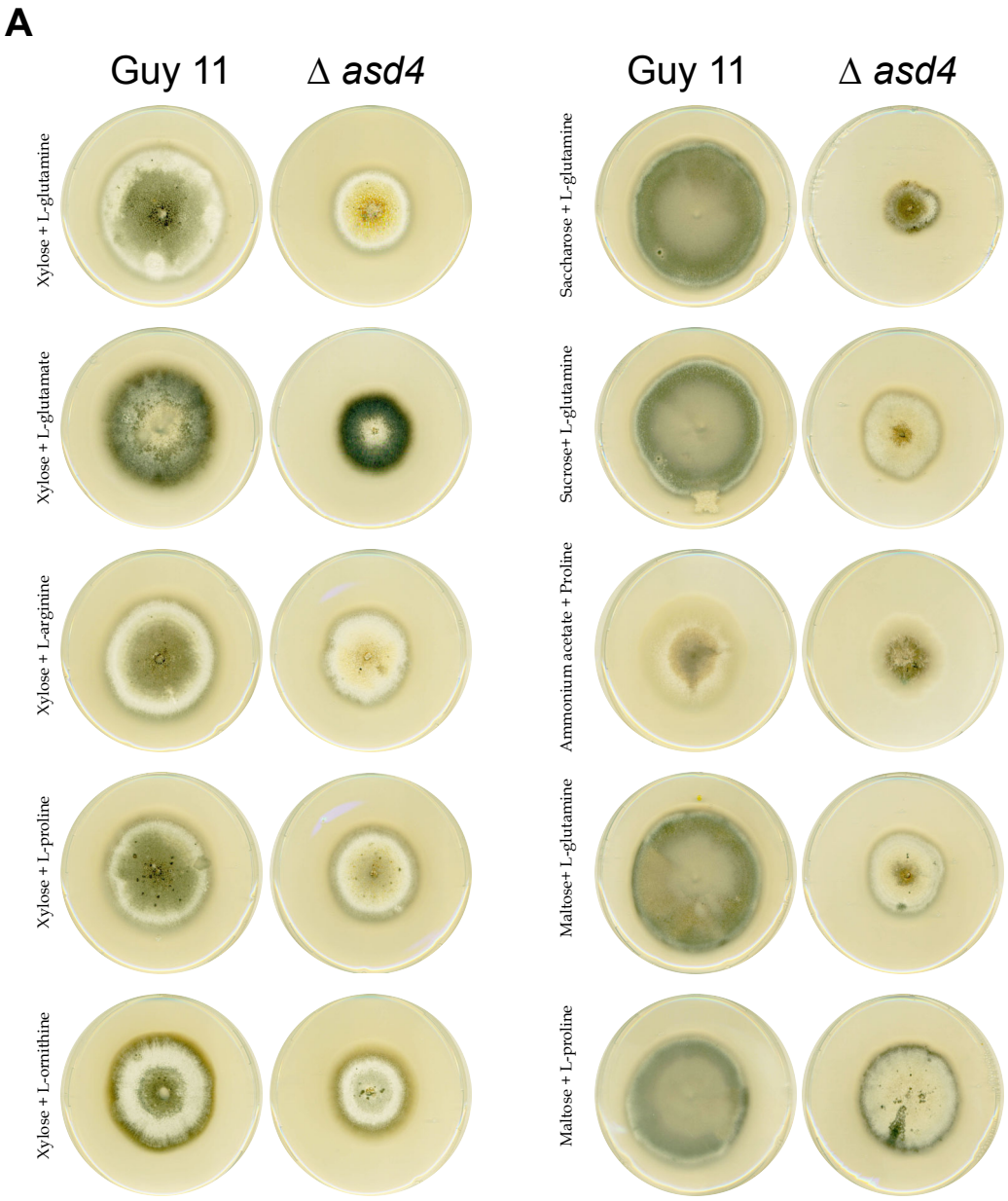

1qaFig. 4. Asd4 negatively regulate the Tor-dependent pathway.

Fig. 5. LC-MS/MS-based proteome profiling of Δ*asd4* strains confirms a role for Asd4 in the regulation of Tor-associated pathways.

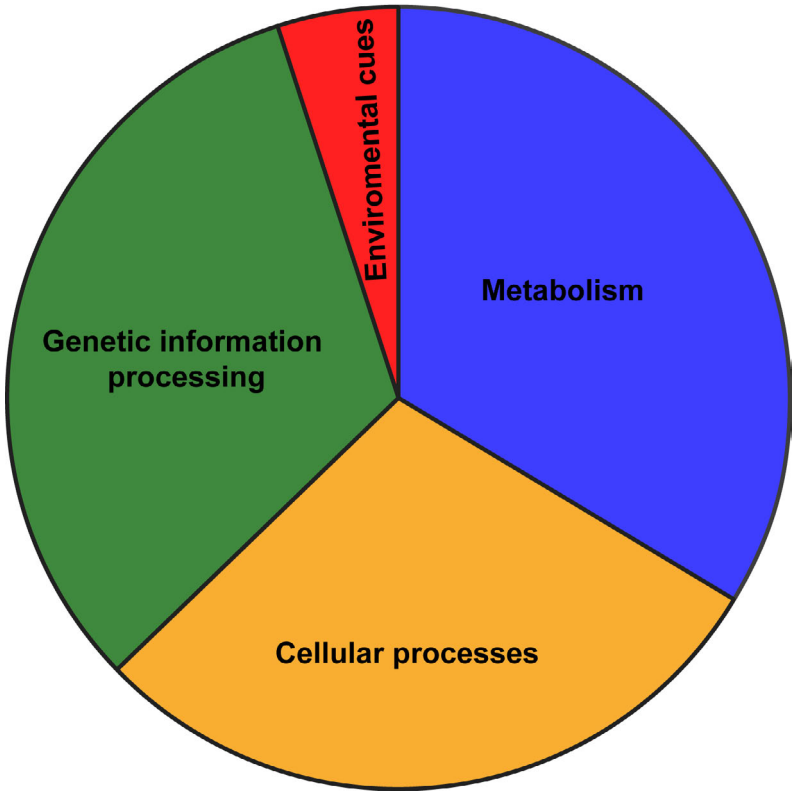

Fig. 6. Asd4 controls autophagy and suggest upregulation of the Tor-dependent pathway.

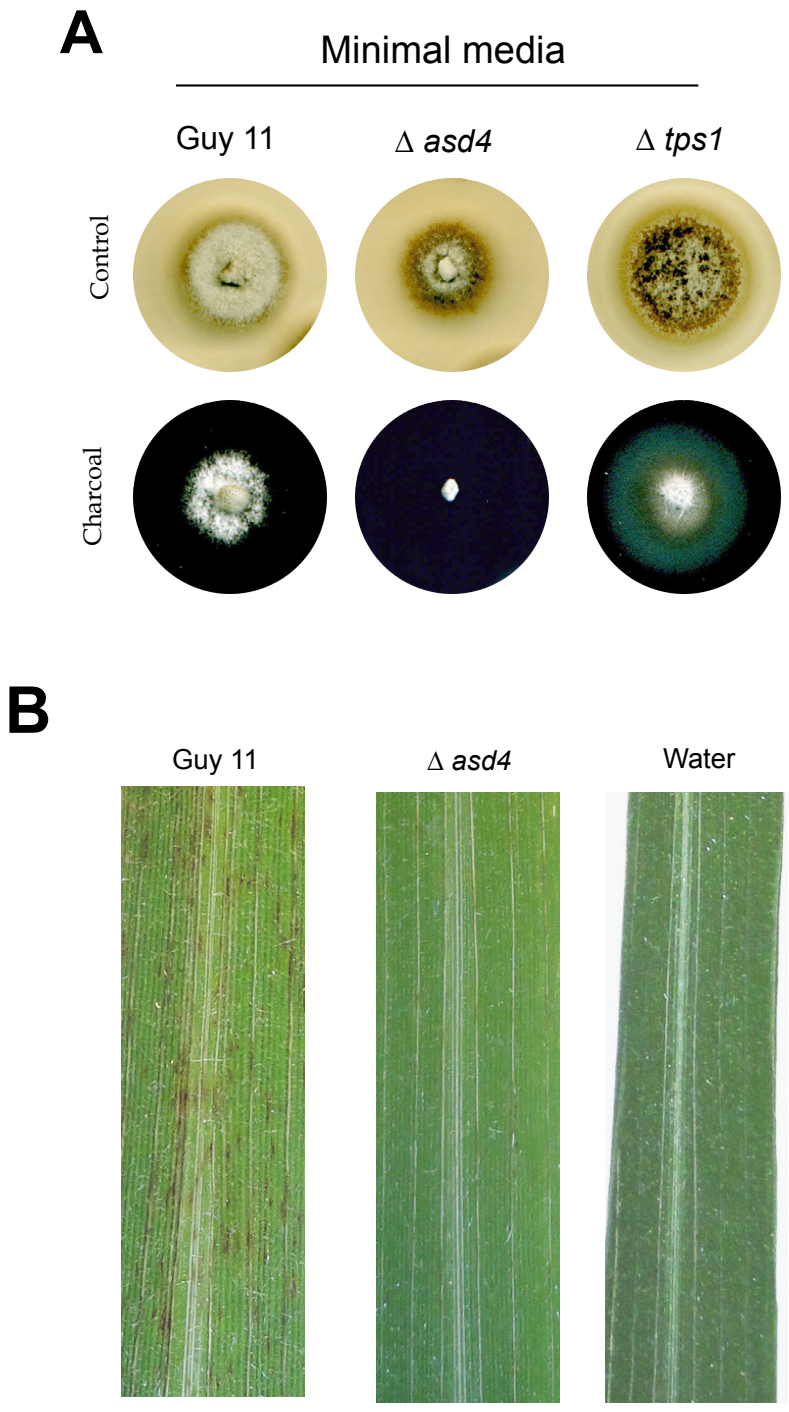

Table S1. LC-MS/MS-based proteome profiling of Δ*asd4* strains**.** Selected 62 proteins that showed at least 2-fold difference in expression between the wild type and the Δ*asd4* mutant strain.

Process	*M. oryzae* ID	Change Asd4 vs Guy11	Increase/Decrease	Gene/Function
Genetic information processing	MGG_06763	present	↑	PriL, primase, synthesize the RNA primers required for DNA replication
	MGG_05129	3-fold	↑	IF-2, translation initiation factor
	MGG_06924	abundant	↑	nucleosome assembly protein
	MGG_07087	8-fold	↑	Syf-1, pre-mRNA splicing factor, DNA repair and transcription protein
	MGG_05676	present	↑	RNase P, generates mature tRNA molecules
	MGG_00019	abundant	↑	SET, methyl transferase, nuclear protein
	MGG_01268	present	↑	RNP, ribonucleoprotein domain, involved in post-transcriptional gene expression
	MGG_06379	present	↑	midasin, maturation and nuclear export of pre-60S ribosome subunits.
	MGG_09907	present	↑	remove ubiquitin molecules from polyubiquinated peptides
	MGG_06462	present	↑	RNA polymerase 2 transcription elongation factor
	MGG_01217	absent	↓	multiple RNA-binding domain-containing protein 1
	MGG_04430	present	↑	Mex67, mRNA export factor, modules signal transduction, pre-mRNA processing and cytoskeleton assembly
	MGG_06038	present	↑	U3, small nucleolar RNA-associated protein
	MGG_15228	present	↑	Replication factor C, involved in DNA replication, repair, modification, and chromatin modelling
	MGG_04486	present	↑	Taz1-interacting factor 1
	MGG_07030	present	↑	ribosomal RNA-processing protein 9
	MGG_05146	absent	↓	ribosomal RNA-processing protein 1
	MGG_12276	absent	↓	DNA damage repair protein
	MGG_03311	absent	↓	activate sequence elements in histone gene promoters
	MGG_09173	absent	↓	deoxyhypusine synthase, posttranslational synthesis of an unusual amino acid
	MGG_11387	absent	↓	RAD50, DNA repair protein
Cellular processes	MGG_11206	present	↑	involved in mitochondrial inner membrane
	MGG_04406	present	↑	26S proteasome non-ATPase regulatory subunit 10
	MGG_05026	absent	↓	S19 , 40S ribosomal protein

	MGG_05062	absent	↓	peroxisomal membrane protein
	MGG_01730	absent	↓	Homeodomain, involved in the transcriptional regulation of key eukaryotic developmental processes
	MGG_11573	present	↑	S10,30S ribosomal protein
	MGG_04179	significanly absent	↓	DBP10, ATP-dependent RNA helicase
	MGG_02252	present	↑	mediate biosynthetic protein transport from the ER, via the Golgi up to the trans Golgi network
	MGG_01034	present	↑	involved in Golgi trafficking
	MGG_10522	present	↑	L1, Ribosomal protein
	MGG_03336	present	↑	LEA domain protein, protect liposomal membrane
	MGG_03755	present	↑	golgi-associated plant pathogenesis related protein
	MGG_04176	present	↑	heterokaryon incompatibility proteins
	MGG_02747	present	↑	S4-A, 40S ribosomal protein, found in stress proteins, ribosomal proteins and tRNA synthetases
	MGG_00457	present	↑	BUD22, ribosome biogenesis
	MGG_00840	2-fold	↑	Rrp14, 60S ribosome biogenesis protein
	MGG_12358	abundant	↑	RGP1-like protein, Retrograde Golgi transport protein
	MGG_07275	4-fold	↑	60S ribosomal protein
Metabolism	MGG_07463	2-fold	↑	D-galacturonic acid reductase, NAD binding Rossmann fold oxidoreductase
	MGG_10910	abundant	↑	Nor-1, aflatoxin biosynthesis ketoreductase
	MGG_05992	present	↑	SO, sulfite oxidase, catalyzes the reaction in the degradation of cysteine and methionine
	MGG_04922	present	↑	alpha-L-arabinofuranosidase and beta-D-xylosidase activity
	MGG_10607	absent	↓	enolase
	MGG_00803	absent	↓	CCR, carbon catabolite-derepressing protein kinase
	MGG_00901	absent	↓	2,3-bisphosphoglycerate-independent phosphoglycerate mutase
	MGG_00832	absent	↓	cytochrome P450
	MGG_11554	absent	↓	Sip1, Raffinose synthase
	MGG_04212	absent	↓	L-ornithine 5-monooxygenase
	MGG_08271	absent	↓	RFT1 , oligosaccharide translocation protein
	MGG_05306	absent	↓	MeaB, bZIP transcription factor, activates nmrA expression
	MGG_13014	present	↑	chitin synthase

	MGG_00969	present	↑	asparagine synthetase 1
	MGG_10606	significanly absent	↓	aminopeptidase 2
	MGG_03181	absent	↓	triose phosphate/phosphate translocator
	MGG_09410	present	↑	thymine dioxygenase
	MGG_05847	2-fold	↓	MFP, facilitate the transport of a variety of substrates e.g. ions, sugar phosphates, amino acids
	MGG_02473	10-fold	↓	ATP, myosin-heavy-chain O-phosphotransferase
	MGG_08724	present	↑	glycosyltransferase
Enviromental cues	MGG_08005	present	↑	Ser/Thr and Tyr protein phosphatases.
	MGG_14008	absent	↓	Ric8 , Guanine nucleotide exchange factor synembryn, regulates neurotransmitter secretion
	MGG_00149	absent	↓	serine/threonine-protein phosphatase PP-Z

Table S2. *Magnaporthe oryzae* strains used in this study.

Strains	Genotype	Reference
Guy11	Wild type	Talbot, 2003.
Δtps1	Trehalose-6-phosphate synthase 1 deletion mutant of Guy11	Foster et al. Wilson et al, 2007; Wilson et al 2010.
Δnut1	Nitrogen metabolite repression mutant of Guy1	Wilson et al, 2010; *This study*.
Δasd4	GATA type transcription factor	Wilson et al, 2010. *This study*.
Δmac1	Adenylate cyclase	Lee et al, 1993.
Δpas2	Gata TF WC-1	This study
Δpas3	Gata TF WC-1	This study
Δrad7	DNA repair	This study
Δgal1P	Galactose-1-phosphate uridylyltransferase	This study
ΔuSDE	Urea carboxylase [EC:6.3.4.6]	This study
Δtwsp	tRNA wybutosine-synthesizing protein 3	This study
Δmt_11	Methyltransferase 11	This study
Δtps1 pas1	Double mutant	This study
Δtps1 asd4	Double mutant	This study